72-22

CNWRA A center of excellence in earth sciences and engineering

A Division of Southwest Research Institute™
6220 Culebra Road • San Antonio, Texas, U.S.A. 78228-5166
(210) 522-5160 • Fax (210) 522-5155

January 28, 2002

U.S. Nuclear Regulatory Commission
ATTN: Dr. Mahendra Shah
NMSS/SFPO
OWFN, Mail Stop 13 D13
Washington, DC 20555

Dear Dr. Shah:

Enclosed are the document requested by the State of Utah in "The State of Utah's Seventeenth Set of Discovery Requests Directed to the NRC Staff." The enclosures include:

1. Copy of Scientific Notebook 353 entries regarding the additional analyses carried out in support of the Supplemental Safety Analysis Report (SSER). These analyses are provided in the scientific notebook because they were not documented in any other paper or report (e.g., Stamatakos et al., 1999-*Seismic Ground Motion at the Private Fuel Storage Facility Site in the Skull Valley Indian Reservation.* San Antonio, TX: Center for Nuclear Waste Regulatory Analyses). I have also added a set of color figures for clarity and a disk with the figures in pdf format.

   a. Comparative analysis of probabilistic hazards results for sites in the western United States used to support SSER conclusions that the Private Fuel Storage (PFS) probabilistic seismic hazard assessment (PSHA) is conservative.

   b. 3DStress™ Analysis performed on the Skull Valley and central Utah fault systems also used to support SSER conclusions that the PFS PSHA is conservative.

2. Copy of the User's Manual for 3DStress™ (version 1.3.3), printed from the HTML files.

For all other document requests, we have determined that all information requested by the state (i) has been provided in previous document requests; (ii) can be obtained from public literature (e.g., scientific journals); (iii) is in the existing PFS docket; or (iv) is in our reports (e.g., Stamatakos et al., 1999, SER, SSER). In particular, the sensitivity calculations referred to by the State in Document Request No. 9 was carried out in support of the original SER and is not new nor has it been updated for the revised SSER. The calculation is documented in Stamatakos et al., (1999).

If you have any additional questions regarding this information, please contact me at (210) 522-5247.

Sincerely,

Dr. John Stamatakos

JS/cap
Attachments

Washington Office • Twinbrook Metro Plaza #210
12300 Twinbrook Parkway • Rockville, Maryland 20852-1606

NMSS01 Public

M. Delligatti
S. Turk
M. Waters
C. Marco
A. Chowdhury
A. Ghosh

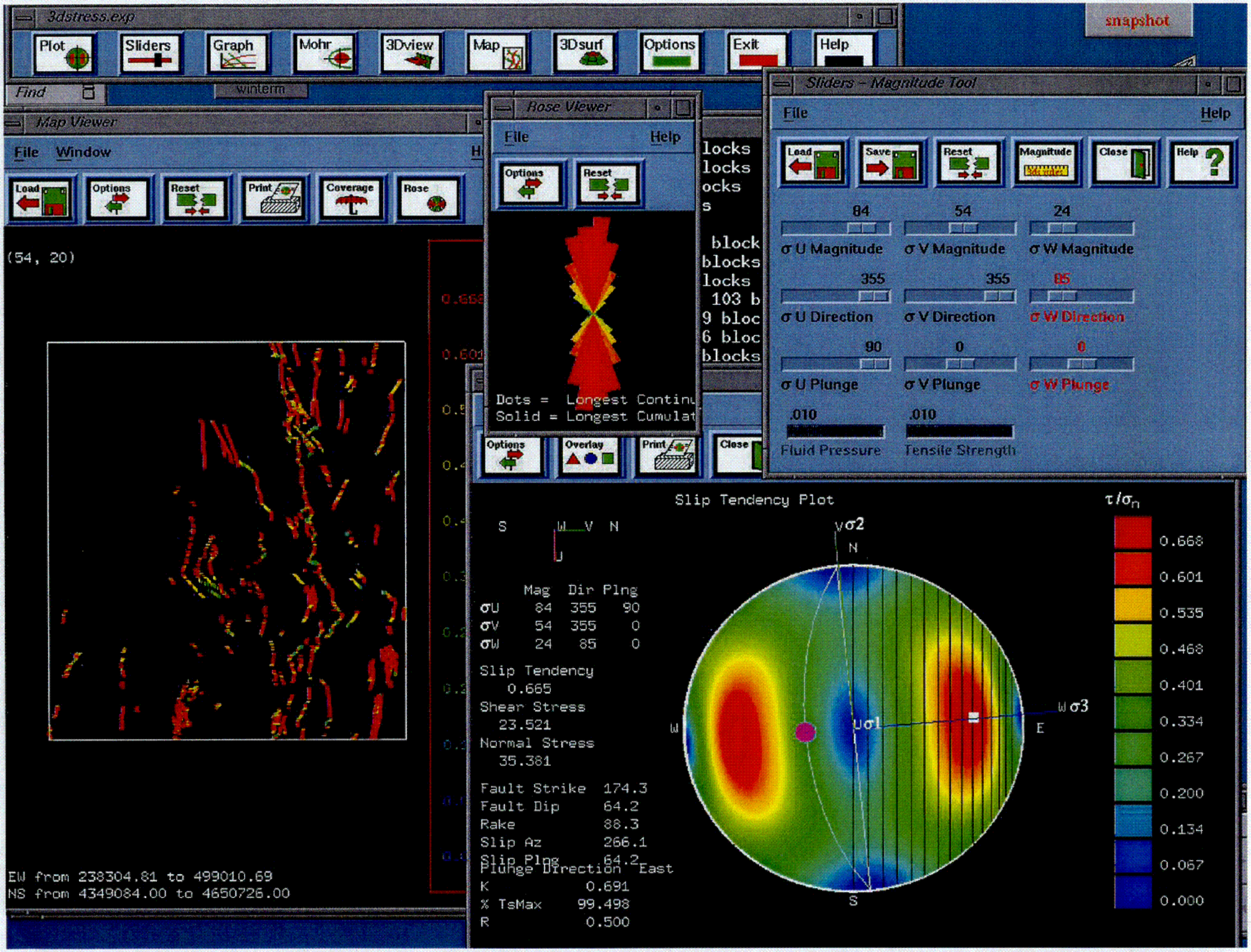
3dstress.exp
Plot
Sliders
Graph
Mohr
3Dview
Map
3Dsurf
Options
Exit
Help
snapshot
Find
winterm
Map Viewer
File Window
Load
Options
Reset
Print
Coverage
Rose
(54, 20)
EW from 238304.81 to 499010.69
NS from 4349084.00 to 4650726.00
Rose Viewer
File
Help
Options
Reset
Dots = Longest Continu
Solid = Longest Cumulat
Overlay
Print
Close
Sliders – Magnitude Tool
File
Help
Load
Save
Reset
Magnitude
Close
Help
84
σ U Magnitude
54
σ V Magnitude
24
σ W Magnitude
355
σ U Direction
355
σ V Direction
85
σ W Direction
90
σ U Plunge
0
σ V Plunge
0
σ W Plunge
.010
Fluid Pressure
.010
Tensile Strength
Slip Tendency Plot
S
W V N
U
Mag Dir Plng
σU 84 355 90
σV 54 355 0
σW 24 85 0
Slip Tendency
0.665
Shear Stress
23.521
Normal Stress
35.381
Fault Strike 174.3
Fault Dip 64.2
Rake 88.3
Slip Az 266.1
Slip Plng 64.2
Plunge Direction East
K 0.691
% TsMax 99.498
R 0.500
Vσ2
N
Uσ1
Wσ3
E
W
S
τ/σn
0.668
0.601
0.535
0.468
0.401
0.334
0.267
0.200
0.134
0.067
0.000

C01

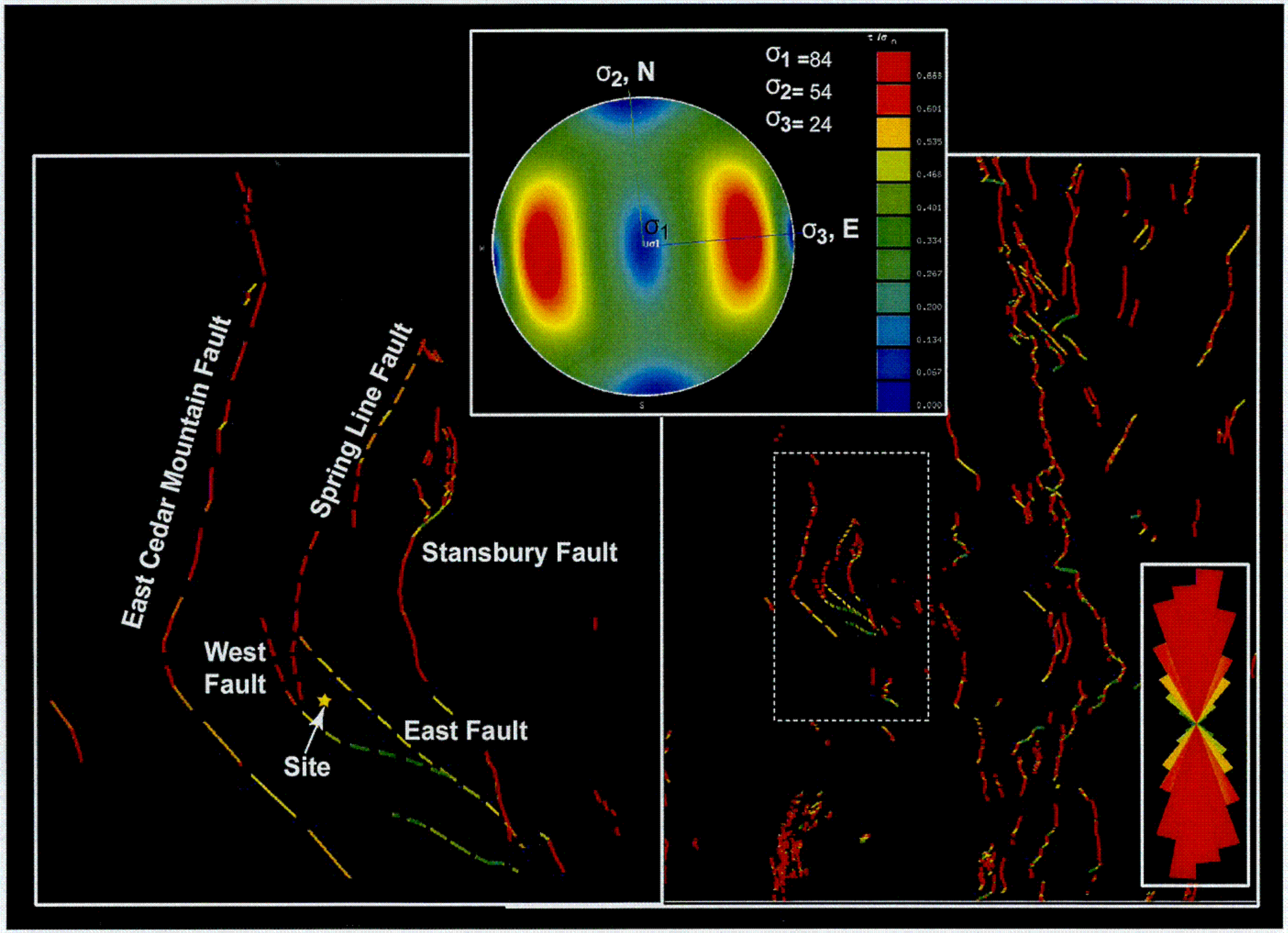
σ2, N
σ1 =84
σ2= 54
σ3= 24
σ1
σ3, E
East Cedar Mountain Fault
Spring Line Fault
Stansbury Fault
West Fault
East Fault
Site

CO2

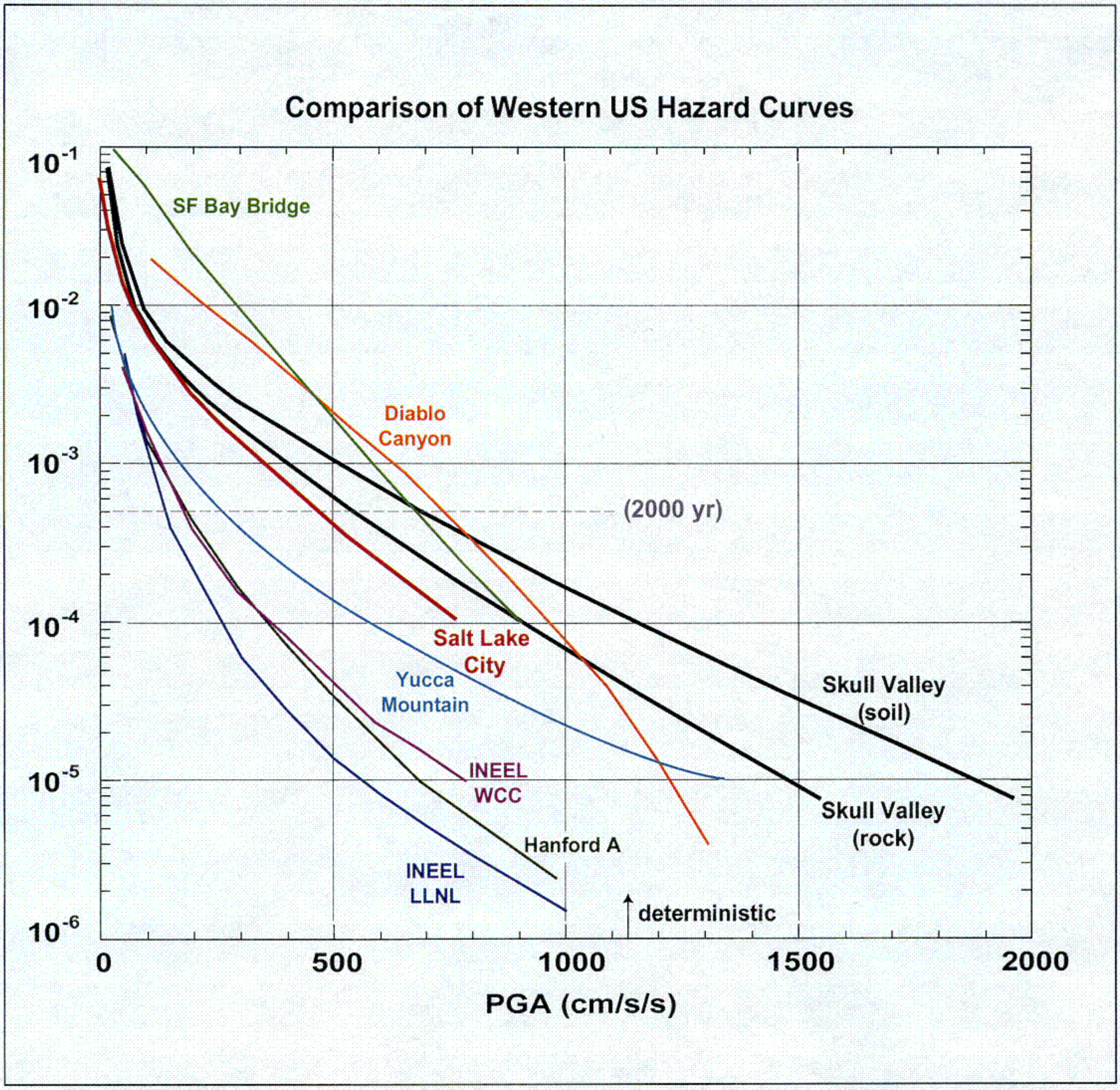

Comparison of Western US Hazard Curves
10-1
10-2
10-3
10-4
10-5
10-6
SF Bay Bridge
Diablo Canyon
(2000 yr)
Salt Lake City
Yucca Mountain
INEEL WCC
Hanford A
INEEL LLNL
Skull Valley (soil)
Skull Valley (rock)
deterministic
0
500
1000
1500
2000
PGA (cm/s/s)

C03

John Stamatakos

353

The Boorum & Pease® Quality Guarantee

The materials and craftsmanship that went into this product are of the finest quality. The pages are thread sewn, meaning they're bound to stay bound. The inks are moisture resistant and will not smear. And the uniform quality of the paper assures consistent rulings, excellent writing surface and erasability. If, at any time during normal use, this product does not perform to your expectations, we will replace it free of charge. Simply write to us:

Boorum & Pease Company
71 Clinton Road, Garden City, NY 11530
Attn: Marketing Services

Any correspondence should include the code number printed at the bottom of this page as well as the book title stamped at the bottom of the spine.

Contents | Page

Scientific Notebook 353 **August 1, 2000**
Initial Entry: John Stamatakos
Project: 20-01405-041 Private Fuel Storage Facility

Title: Evaluation of PFS Earthquake Analyses for SER on PFSF License Application (SAR)

The entries in this notebook document work done in support of the staff evaluation of the PFS seismic hazard studies for the NRC Safety Evaluation Report (SER) on the Utah PFSF License Application (SAR) and supporting document titled "*Seismic Motion and faulting hazard at Privfate Fuel Storage Facility in the Skull Valley Indian Reservation, Toelle County, Utah.*"
JS 8/1/2000

Dr. John Stamatakos, Ph.D. - CNWRA Senior Research Scientist
Dr. Rui Chen - CNWRA Senior Research Scientist
Mr. Peter La Femina - CNWRA Research Scientist

Dr. Martin McCann, Ph.D. - Consultant, Jack R Benjamin and Associates, Menlo Park, California

December 18, 2001

Note: All data and reviews pertaining to this project to date are documenting in CNWRA reports (Draft and Final SER, and Stamatakos et al., 1999).No additional calculations or analyses were permed in support of these documents that required entry into this Scientific Notebook. In support of the review of the Supplemental SER, we carried out two additional analyses. These additional analyses will be added to the revision of the Stamatakos et al (1999) report if a revision is published. Current schedule for hearings on the seismic issues may preclude revision of that report. Thus, the additional analysis were added to this notebook for proper QA documentation.

12/18/01

Scientific Notebook 353
December, 18, 2001
Entry By: John A. Stamatakos

Purpose: To document comparison of Private Fuel Storage Facility (PFS) probabilistic seismic hazard results (PSHA) to other PSHA results for the western United States.

Investigator: John A. Stamatakos

Background Information

In the revisions to the SAR by the applicant completed in the Spring of 2001, the seismic hazard increased by a large amount. The large increase in the hazard appears to be primarily from a revision to the site response models. For example the peak ground acceleration for the 2000 yr return period rose 35% from0.528 g to 0.711g. The following Table summarizes some of the changes in spectral acceleration.

Comparison of PSHA for 2,000-yr Return Period Spectral Acceleration (with 5% Damping)

Period (sec)	Horizontal Ground Motion (g)		Vertical Ground Motion (g)	
	SAR Revision 22	**SAR Revision 18 (former design)**	**SAR Revision 22**	**SAR Revision 18 (former design)**
PGA	0.711	0.528	0.695	0.533
0.1	1.541	1.046	1.752	1.369
0.5	1.045	1.166	0.509	0.476
2.0	0.164	0.272	0.088	0.088

Data and Procedure:

1. To assess these ground motion results, I plotted the hazard curves for the Skull Valley site against PSHA hazard curves for other sites in the western United States. The skull valley data were provided to me on disk within the responses to RAI package following the March, 2001 meeting in San Antonio.

A set of seven hazard curves were provided to me from Dr. M. McCann n September, 30, 2001. Dr. McCann indicated that the data were from 1993.

The following table is a printout of the Excell work sheet of the data provided to me by Dr. McCann.

Peak ground Accelerations for Seven Western United States Sites

No.	Site	Ground Motion/ Curve Type												
1	SF Bay Bridge	PGA (cm/s/s)	34.34	98.1	196.2	392.4	588.6	784.8	912.33					
		Mean	1.00E01	6.00E02	2.22E02	4.81E03	1.00E03	2.35E04	1.00E04					
2	Diablo Canyon	PGA (cm/s/s)	109	218	327	436	546	654	763	872	981	1090	1199	1308
		80th Fractile	2.00E02	1.08E02	6.00E03	3.16E03	1.63E03	9.00E04	4.33E04	2.00E04	9.00E05	3.94E05	1.33E05	4.00E06
3	Los Alamos Site 1	PGA (cm/s/s)	55.9	77.5	98.1	196.2	294.3	343.35	392.4	600.37				
		Mean	8.51E03	5.44E03	3.30E03	8.95E04	2.80E04	1.85E04	1.04E04	1.00E05				
4	Hanford Site A	PGA (cm/s/s)	19.62	98.1	196.2	294.3	392.4	490.5	686.7	981				
		Mean	8.58E03	1.44E03	4.41E04	1.70E04	7.59E05	3.66E05	1.00E05	2.42E06				
5	INEL 1 (LLNL)	PGA (cm/s/s)	50	80	150	250	300	400	500	600	700	800	1000	
		Mean	5.00E03	2.00E03	4.00E04	1.16E04	6.03E05	2.82E05	1.37E05	8.41E06	5.32E06	3.14E06	1.53E06	
6	INEL 1 (WCC)	PGA (cm/s/s)	49.05	98.1	196.2	294.3	392.4	490.5	588.6	686.7	784.8			
		Mean	4.16E03	1.58E03	4.00E04	1.58E04	8.48E05	4.48E05	2.42E05	1.58E06	1.00E06			
7	PALO VERDE	PGA (cm/s/s)	10	20	50	70	100	150	200	300	500	1000		
		Mean	3.50E02	7.20E03	1.00E03	5.40E04	2.80E04	1.30E04	6.90E05	2.10E06	3.10E06	2.10E07		

SF Bay Bridge - Geomatrix Consultants, Inc., PSHA for the San Francisco Bay Bridge, prepared for the California Department of Transportation.

Diablo Canyon - Pacific Gas and Electric Company, "Final Report of the Diablo Canyon Long Term Seismic Program," Docket Nos. 50-275 and 50-323, San Francisco, CA, July 1988.

Los Alamos Site 1 - Woodward Clyde Consultants, Inc., PSHA for the Los Alamos Site, New Mexico, date unknown.

Hanford Site A - Geomatrix Consultants, Inc., "Seismic Hazards Assessment for WNP-3, SATSOP Washington," prepared for Washington Public Power Supply System, Richland, WA, date unknown.

INEL 1 (LLNL) - Lawrence Livermore National Laboratory, date unknown.

INEL 1 (WCC) - Woodward Clyde Consultants, Inc., PSHA for the INEL Site, Idaho, date unknown.

Palo Verde - Risk Engineering, Inc., PSHA for the Palo Verde Nuclear Power Plant Site, Arizona, date unknown.

2. In addition to the data provided to me by Dr. McCann, I gather one additional seismic hazard curve from a publication I found on the web published by the United States geological Survey

Frankel, A., S. Harmsen, C. Mueller, T. Barnhard, E.V. Leyendecker, D. Perkins, S. Hanson, N. Dickman, M. Hopper. 1997. *USGS National Seismic Hazard Maps: Uniform Hazard Spectra, De-aggregation, and Uncertainty*, Proceedings of FHWA/NCEER Workshop on the National Representation of Seismic Ground Motion for New and Existing Highway Facilities, NCEER Technology Report 97-0010, pp. 39-73, http://geohazards.cr.usgs.gov/eq/uncertainties/nceer.html).

The following figure (figure 3) is from that paper. From the figure I digitized values for the Salt Lake City Hazard curve, and converted them to cm/s/s 1 g = 9.8 m/s/s = 980 cm/s/s).

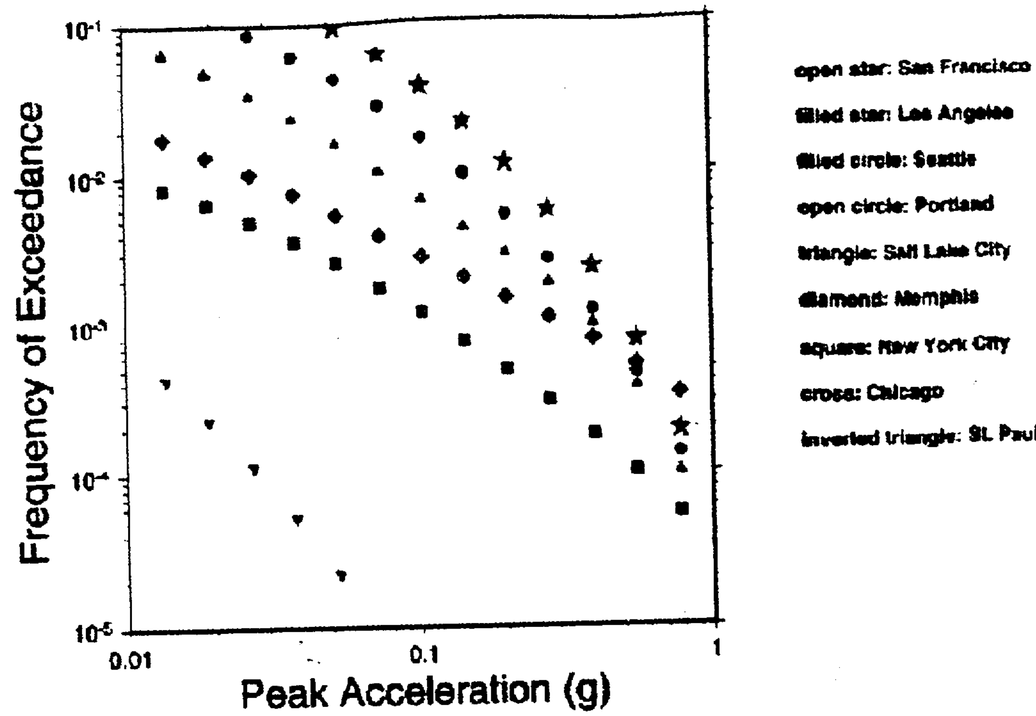

Figure 3. Mean hazard curves for selected cities.

Table of PGA values derived from Frankel et al (1997) curve.

PGA (cm/s/s)	Probability
0	0.064
18.62	0.052
23.52	0.0325
36.26	0.0225
49.98	0.014
73.5	0.01
107.8	0.0064
127.4	0.0042
205.8	0.0028
264.6	0.00175
392	0.00095
529.2	0.00035
764.4	1.00E-04

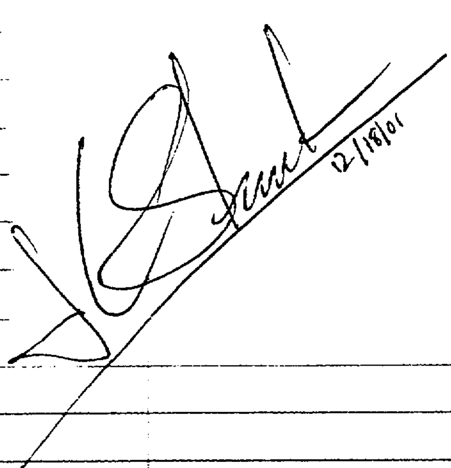

3. I then plotted all the data (using Kaleida Graph, version 3.09) to produce the following graph.

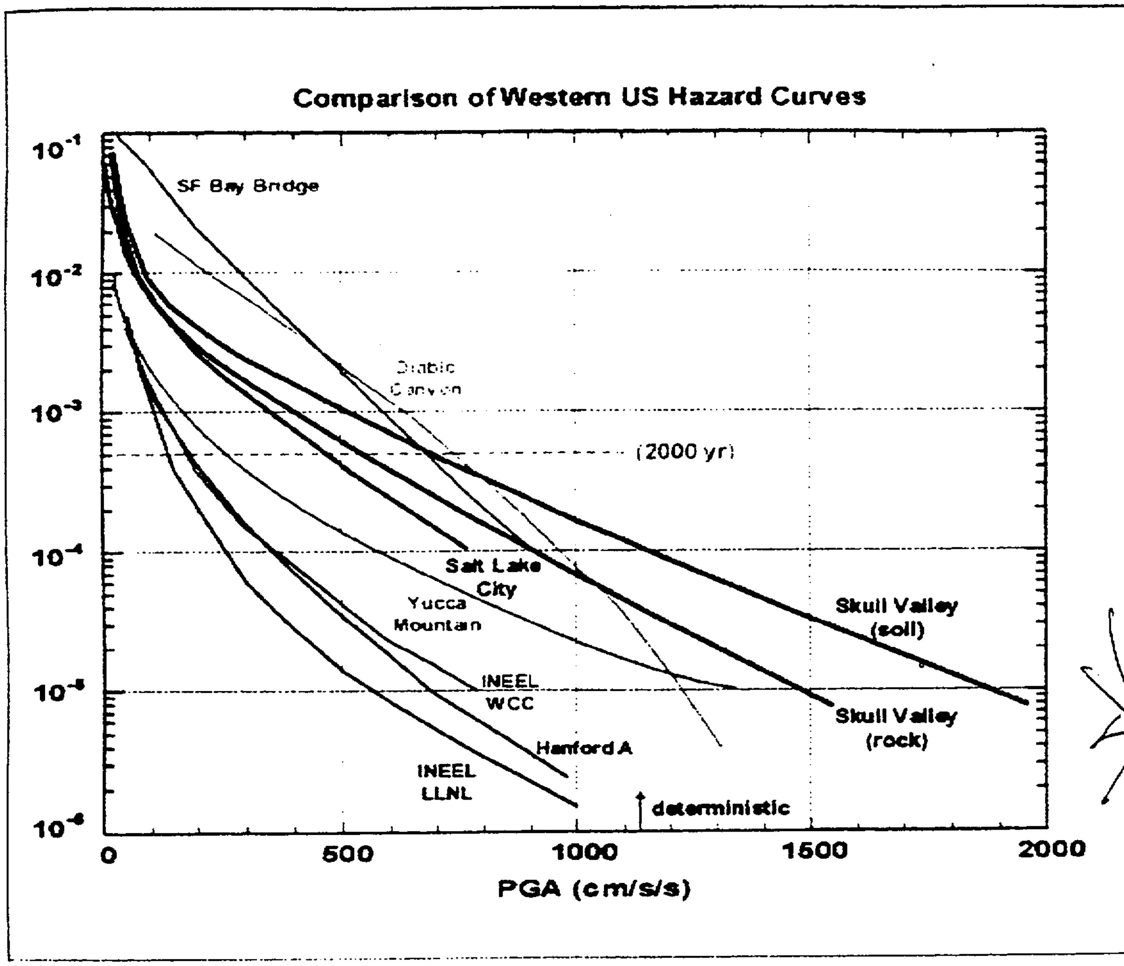

4. Based on deposition testimony by the State during October, 2001, I learned of a seismic hazard study completed by Dames and Moore in 1996 as part of the I-15 Corridor construction project.

Dames & Moore, Inc. 1996. *Final Report Seismic Hazard Analysis of the I-15 Corridor 10600 South to 500 North Salt Lake County, Utah*. UT-47026. Report submitted to Parsons Brinckerhoff. Salt Lake City, UT: Dames & Moore.

In that report, table 4.3 on p. 4-9 provides a summary of PGA values for 9 sites along the I-15 interstate highway corridor for probabilities of exceedence values at approximately 500, 1000, and 2500 yrs. Those values (mean) are:

Site	PGA (mean)
	2500 yr
PB-1	0.654
PG17DhR-15A	0.686
PG17DH-7A	0.674
PB-2	0.65
PB-3	0.602
PB-4	0.575
PB-5	0.566
PG17DH-16A	0.562
PG17DH-17A	0.561

12/18/01

Discussion

The results show the conservative nature of the applicant's source characterization and PSHA results presented in the SAR. This conservatism is evident when the results are compared to PSHA results for other sites in Utah, especially those in and around Salt Lake City. This a comparison shows that the seismic hazard in Skull Valley was calculated by the applicant to be higher than seismic hazard estimates that have been performed for sites at, or near, Salt Lake City, despite the fact that fault sources near Salt Lake City are larger and more active than fault sources near the PFS site. For example, the results of the applicant's PSHA for Skull Valley (Geomatrix Consultants, Inc., 2001a) suggest that it is 1.5 times more likely that a ground motion of 0.5g horizontal peak ground acceleration or greater will be exceeded at the PFS site (assuming hard rock site conditions), than at Salt Lake City, based on the USGS National Earthquake Hazard Reduction Program (Frankel et al., 1997).

Similarly, the 2000-yr horizontal peak ground acceleration for Skull Valley (soil hazard) as estimated by the applicant, is higher than the 2500-yr ground motions for the nine sites along the Wasatch Front that were evaluated as part of the Utah Department of Transportation I-15 Reconstruction Project (Dames & Moore, Inc., 1996). The ground motions estimated by the applicant in Skull Valley are higher than those for the I-15 corridor, despite the close proximity of Salt Lake City to the Wasatch fault, which has a slip rate nearly ten times larger than the Stansbury or East Faults (cf., Martinez et al., 1998; Geomatrix Consultants, Inc., 1999a) and is capable of producing significantly larger magnitude earthquakes than the faults near the PFS Facility site in Skull Valley (cf., Machette et al., 1991; Geomatrix Consultants, Inc., 1999a).

Geomatrix Consultants, Inc. 1999a. *Fault Evaluation Study and Seismic Hazard Assessment Private Fuel Storage Facility, Skull Valley, Utah.* San Francisco, CA: Geomatrix Consultants, Inc.

Machette, M.N., S.F. Personius, A.R. Nelson, D.P. Schwartz, and W.R. Lund. 1991. *The Wasatch fault zone, Utah-segmentation and history of Holocene earthquakes.* Journal of Structural Geology 13: 137-149.

Martinez, L., C. M. Meertens, and R. B. Smith. 1998. *Anomalous intraplate deformation of the Basin and Range-Rocky Mountain transition from initial GPS measurements,* Geophysical Research. Letters 24: 2741-2744.

Scientific Notebook 353
December, 18, 2001
Entry By: John Stamatakos

Purpose: Document Slip Tendency Analysis for Supplemental Safety Evaluation Report, Private Fuel Storage, Skull Valley, Utah.

Investigator: John A Stamatakos

Background Information

The previous entry shows concludes that the ground motion hazard for Skull Valley, as estimated by the applicant, is conservative. To assess potential conservatism in the applicant's calculations I performed a slip tendency analysis of the Skull Valley Site using the computer program 3DStress™ (version 1.3.3). The aim of the analysis was to determine if the faults in Skull Valley are in optimal orientations for future slip, given what is known about the current stress conditions in this part of the earth's crust in Utah. Specifically, I wanted to determining if assumptions made by the applicant about rupture initiation and fault length or fault segmentation led to overestimation of the ground motion hazard.

Procedures

The faults from Skull Valley and Central Utah (including the Wasatch fault) were digitized from maps provided in the SAR and rectified in Arcview (verison3.1). The digital files were then exported to 3dStress™. I then asked Dr. David Ferrill and Dr. Alan Morris to run the program for me to assess slip tendency values. The analysis was performed on October 11, 2001.

The slip tendency analysis (Morris et al., 1996) was completed using an interactive stress analysis program (3DStress™) that assesses potential fault activity relative to crustal stress. For Skull Valley, the stress tensor is defined with a vertical maximum principal stress (σ_1), a horizontal intermediate principal stress (σ_2) with azimuth of 355°, and a horizontal minimum principal stress (σ_3) with an azimuth of 085°. The stress magnitude ratios are $\sigma_1/\sigma_3 = 3.50$ and $\sigma_1/\sigma_2 = 1.56$. This orientation for the principal stresses was based on recent global positioning satellite information (Martinez, et al., 1998a). The slip tendency analysis assumed a normal-faulting regime, with rock density equal to 2.7 g/cc, fault dip equal to 60°, water table at a depth of 40 m, and a hydrostatic fluid pressure gradient.

Software:

3DStress v.1.3.3

Stress Tensor Assumptions:

(i) Rock density = 2.7 g/cc
(ii) Water table depth = 40 m
(iii) Stress tensor calculated for depth of 5 km.
(iv) Fluid pressure gradient is hydrostatic
(v) Maximum slip tendency must be sufficient to produce slip on ideally oriented faults (Ts max

greater than or equal to 0.67)

(vi) Normal faulting stress regime - σ_1 vertical, lithostatic

(vii) Faults dip 60°

(viii) Magnitude of intermediate principal stress is centered between max and min principal stresses

Effective Stress Tensor (corrected for fluid pressure):

Effective σ_1 = vertical, 84 Mpa
Effective σ_2 = azimuth 355, 54 Mpa
Effective σ_3 = azimuth 085, 24 MPa

Martinez, L., C. M. Meertens, and R. B. Smith. 1998. *Anomalous intraplate deformation of the Basin and Range-Rocky Mountain transition from initial GPS measurements,* Geophysical Research. Letters 24: 2741-2744.

Morris, A., D.A. Ferrill, and D.B. Henderson. 1996. *Slip-tendency analysis and fault reactivation.* Geology 24, 275-278.

The following two pages are figures from 3DStress™ that summarize the slip tendency results. The first figure is an electronic snapshot of the screen showing the results of the analysis. The second figure is a summary shot showing a close-up of Skull Valley along site the central Utah regional map.

12/18/01

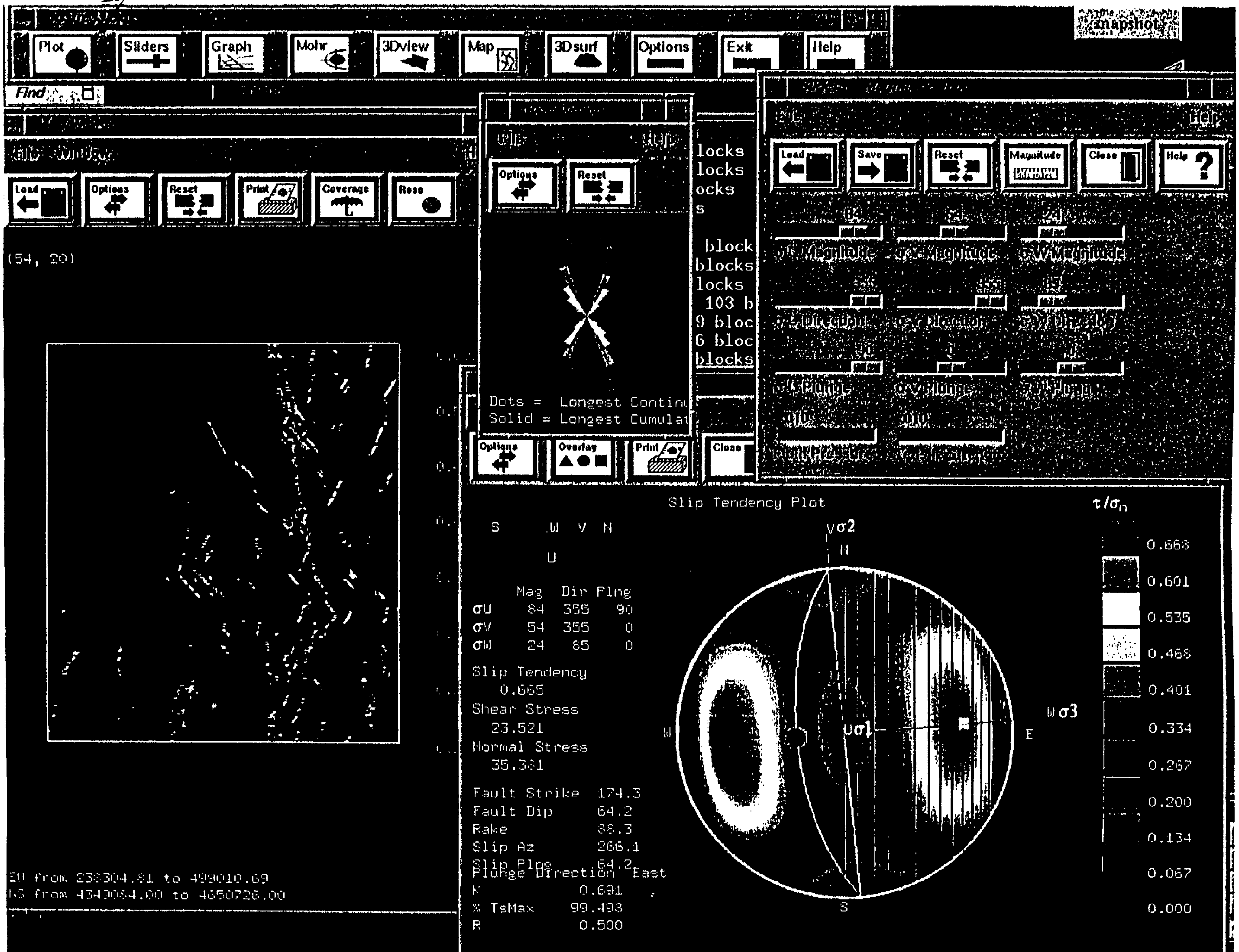
Plot
Sliders
Graph
Mohr
3Dview
Map
3Dsurf
Options
Exit
Help
snapshot
Find
Load
Options
Reset
Print
Coverage
(54, 20)
Options
Reset
Dots = Longest Contin
Solid = Longest Cumulat
locks
locks
ocks
block
blocks
blocks
locks
103 b
9 bloc
6 bloc
blocks
Load
Save
Reset
Magnitude
Close
Help
Options
Overlay
Print
Close
Slip Tendency Plot
S W V N
U
Mag Dir Plng
σU 84 355 90
σV 54 355 0
σW 24 85 0
Slip Tendency
0.665
Shear Stress
23.521
Normal Stress
35.381
Fault Strike 174.3
Fault Dip 64.2
Rake 88.3
Slip Az 266.1
Slip Plng 64.2
Plunge Direction East
0.691
% TsMax 99.493
R 0.500
Vσ2
N
W
Uσ1
E
Wσ3
S
τ/σn
0.668
0.601
0.535
0.468
0.401
0.334
0.267
0.200
0.134
0.067
0.000
EW from 238304.81 to 498010.69
NS from 4340064.00 to 4650728.00

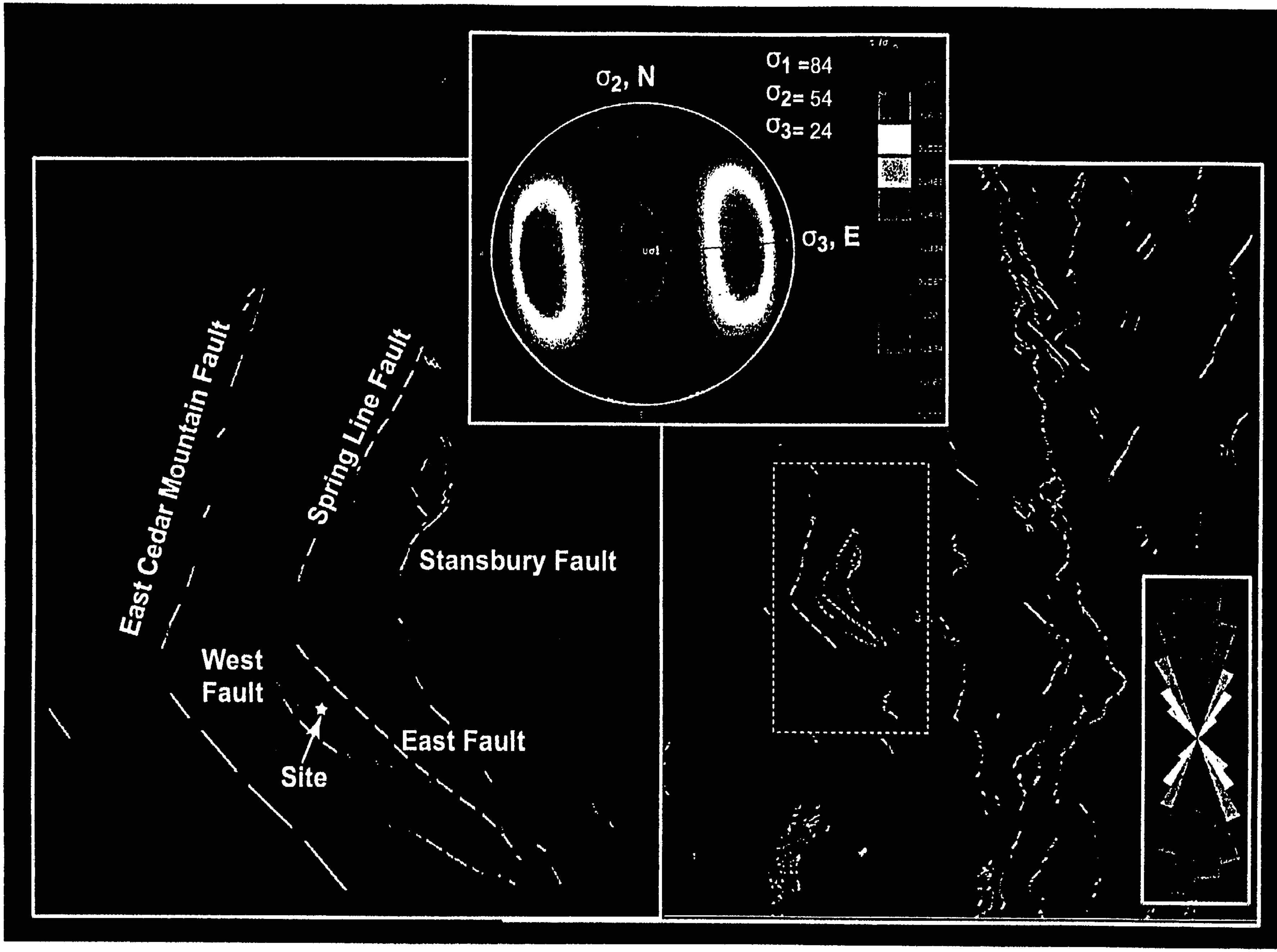
σ2, N
σ1 =84
σ2= 54
σ3= 24
σ3, E
East Cedar Mountain Fault
Spring Line Fault
Stansbury Fault
West Fault
East Fault
Site

Discussion

In slip tendency analysis, the underlying assumption is that the regional stress state controls slip tendency and that there are no significant deviations due to local perturbations of the stress conditions. This assumption is supported by a similar slip tendency analysis of the Wasatch fault, which shows highest slip tendency values for the segments of the fault considered to be most active (Machette et al., 1991).

The slip tendency analysis shows that segments of the East fault and the East Cedar Mountain fault nearest the PFS site have relatively low slip tendency values compared to segments farther north in Skull Valley. As discussed in the following sections on site-to-source distances and maximum magnitudes, these results indicate that the seismic source characterization of the PSHA study conducted by Geomatrix Consultants, Inc. (1999a, and 2001a) is conservative. Three areas of conservatism are the distribution of site-to-source distance, maximum magnitude earthquakes, and potential of the West fault as a seismogenic source (discussed in Stamatakos et al., 1999).

Distributions of Site-to-Source Distances

Results of the slip tendency analysis indicate that fault segments with approximately North-South strikes (azimuth = 175°) are optimally oriented for future fault slip. Faults with north northeast-south southwest strikes have high slip tendency values. In contrast, fault segments with northwest-southeast strikes, such as the East fault near the PFS Facility site and the southern segments of the East Cedar Mountain fault also near the PFS Facility site, have relatively low slip tendency values. Therefore, these fault segments are less likely to slip in the future than fault segments further from the site. Fault rupture close to the site greatly influence the seismic hazard. The closer the earthquake is to the site, the larger the resulting ground motions compared to an equal magnitude earthquake on a fault segment farther away from the site.

In the site-to-source distributions used in the ground motion attenuation equations, Geomatrix Consultants, Inc. (1999a) assumed uniform distributions of earthquake ruptures along active fault segments. Given the slip tendency analysis described above, this assumption by Geomatrix Consultants, Inc. (1999a) is conservative. The staff concludes that seismic source models that incorporate slip tendency would result in a lower ground motion hazard than the one developed by the applicant.

Maximum Magnitude

The slip tendency results suggest that Geomatrix Consultants, Inc. (1999a) may have overestimated the maximum magnitude of the East and East Cedar Mountain faults near the PSFS site. In the SAR, the applicant first developed conceptual models of the physical dimensions of fault rupture—either rupture area or trace length of surface fault rupture—based on the geologic record (Geomatrix Consultants, Inc.,1999a). Second, the applicant developed distributions of maximum magnitudes for each active fault using empirical scaling relationships developed from the magnitudes and associated rupture dimensions of historical earthquakes (e.g., Wells and Coppersmith,1994). In developing the fault segment models, the applicant conservatively assumed that the entire mapped length of the surface trace length represents active fault segments. Thus, these maximum fault dimensions produce conservative estimates of maximum magnitude.

The slip tendency analysis indicates that parts of the East and East Cedar Mountain faults near the

PFS Facility site have relatively low slip tendency values. Thus, these faults may be smaller tha in the fault models used by the applicant to estimate maximum magnitude. Fault rupture mode developed using slip tendency analysis would therefore lead to fault segment models with small rupture dimensions (length or area) than those used by Geomatrix Consultants, Inc. (1999a) Because distributions of maximum magnitude for each active fault are derived from empiric scaling relationships of rupture area or rupture length (e.g., Wells and Coppersmith,1994 application of the slip tendency analysis would thereby result in smaller predicted maximu magnitudes than those developed by the applicant. Smaller maximum magnitudes would reduc the overall ground motion hazard.

In summary, the staff found that the applicant's considerations of seismic source characteristic and associated uncertainties provide reasonable assurance that all significant sources of futur seismic activity have been identified and their characteristics and associated uncertainties ar adequately or conservatively described and appropriately included in the evaluation of the seismi ground motion hazard. Stamatakos et al. (1999) provides more details of PFS's seismic sourc characterization and the staff's independent sensitivity analyses.

Geomatrix Consultants, Inc. 1999a. *Fault Evaluation Study and Seismic Hazard Assessment Private Fuel Storag Facility, Skull Valley, Utah.* San Francisco, CA: Geomatrix Consultants, Inc.

Machette, M.N., S.F. Personius, A.R. Nelson, D.P. Schwartz, and W.R. Lund. 1991. *The Wasatch fault zone, Utah segmentation and history of Holocene earthquakes.* Journal of Structural Geology 13: 137-149.

Stamatakos, J., R. Chen, M. McCann, and A.H. Chowdhury. 1999. *Seismic Ground Motion at the Private Fuel Storag Facility Site in the Skull Valley Indian Reservation.* San Antonio, TX: Center for Nuclear Waste Regulator Analyses.

Wells, D.W., and K.J. Coppersmith. 1994. New empirical relationships among magnitude, rupture length, rupture width, rupture area, and surface displacement. *Bulletin of the Seismological Society of America* 84: 974–1,002

2/15/01

User's Guide for Version 1.3.3

3DStress was prepared as an account of work performed by the Center for Nuclear Waste Regulatory Analyses (CNWRA) for the Division of Waste Management of the Nuclear Regulatory Commission (NRC), an independent agency of the United States Government. Neither the developer(s) of 3DStress nor any of their sponsors make any warranty, expressec or implied, or assume any legal liability or responsibility for the accuracy, completeness, or usefulness of any information, apparatus, product or process disclosed, or represent that its use would not fringe on privately-owned rights.

Technical Support

For technical support for 3DStress contact:

Dr. David A. Ferrill, CNWRA, Southwest Research Institute, 6220 Culebra Road, San Antonio Texas 78238 USA, 210-522-6082 (voice), 210-522-5155 (fax), E-mail: dferrill@swri.edu

Hardware Requirements

Sun Ultra Workstation Running Solaris 2.7 Operating System

Overview

3DStress is a tool for computing the propensity for a fault to slip or dilate based on three-dimensional (3D) stress conditions. **Slip** tendency is a ratio of the shear stress τ divided by the normal stress (σ_n) on a fault surface, as shown in the equation below:

$$\text{Slip tendency} = \tau / \sigma_n$$

The stress axis with the **greatest** magnitude is called σ_1. The stress axis with the **smallest** magnitude is called σ_3. The **intermediate** stress axis is called σ_2. Any of the stress axes $(\sigma_u, \sigma_v, \text{or } \sigma_w)$ can be σ_1, σ_2 or σ_3 depending on the user selection.

Dilation tendency is the relative propensity for a fault to dilate based on the 3D stress conditions and is computed as shown in the equation below:

$$\text{Dilation tendency} = (\sigma_1 - \sigma_n) / (\sigma_1 - \sigma_3)$$

Leakage factor is a quantitative estimate of the propensity for a fault or fracture to dilate, for situations where fluid pressure and fault or fracture tensile strength are known or can be inferred. Leakage factor is computed as a function of pore fluid pressure $(P_f), \sigma_n$, and tensile strength (T) by the equation below:

$$\text{Leakage factor} = P_f / (\sigma_n - T)$$

Helpful Hint: 3DStress is memory intensive, especially with large data files; it will perform more smoothly in short sessions. Try to exit 3DStress and restart before moving from one project to the next to give it the chance to start with the maximum amount of memory and swap space available.

For additional background and details on slip tendency see the following references:

Morris, A., D. A. Ferrill, and D. B. Henderson, 1996, "Slip-tendency analysis and fault reactivation," Geology, March 1996, 24(3): 275-278.

Morris, A. P., D. A. Ferrill, and D. B. Henderson, 1994, "Slip tendency analysis and fault reactivation," EOS, Transactions of the American Geophysical Union, 75(44): 591.

Ferrill, D. A., S. R. Young, A. P. Morris, D. B. Henderson, and R. H. Martin, 1994, "3-Dimensional stress domains interpreted from fault slip patterns in southern Society of America Abstracts with Programs, 26(7): A185.

Ferrill, D. A., A. P. Morris, D. B. Henderson, and R. H. Martin, 1994, "Tectonic processes in the Central Basin and Range region," NRC High-Level Radioactive Waste Research at

CNWRA, July-December, 1994. CNWRA 94-02S. 121-139.

Ferrill, D. A., A. P. Morris, S. M. Jones, and J. A. Stamatakos, 1998, "Extensional Layer-Parallel Shear and Normal Faulting," Journal of Structural Geology, 20(4): 355-362.

Ferrill, D. A., James, Winterle, Gordon Wittmeyer, Darrell Sims, Shannon Colton, Amit Armstrong, and Alan P. Morris, 1999, "Stressed Rock Strains Groundwater at Yucca Mountain, Nevada," GSA Today, 9(5): 1-8

Starting 3DStress

To start 3DStress from a shell window, change directories to the directory with the executable for 3DStress and enter:

% 3dstress

Two windows similar to the ones below will appear on the display.

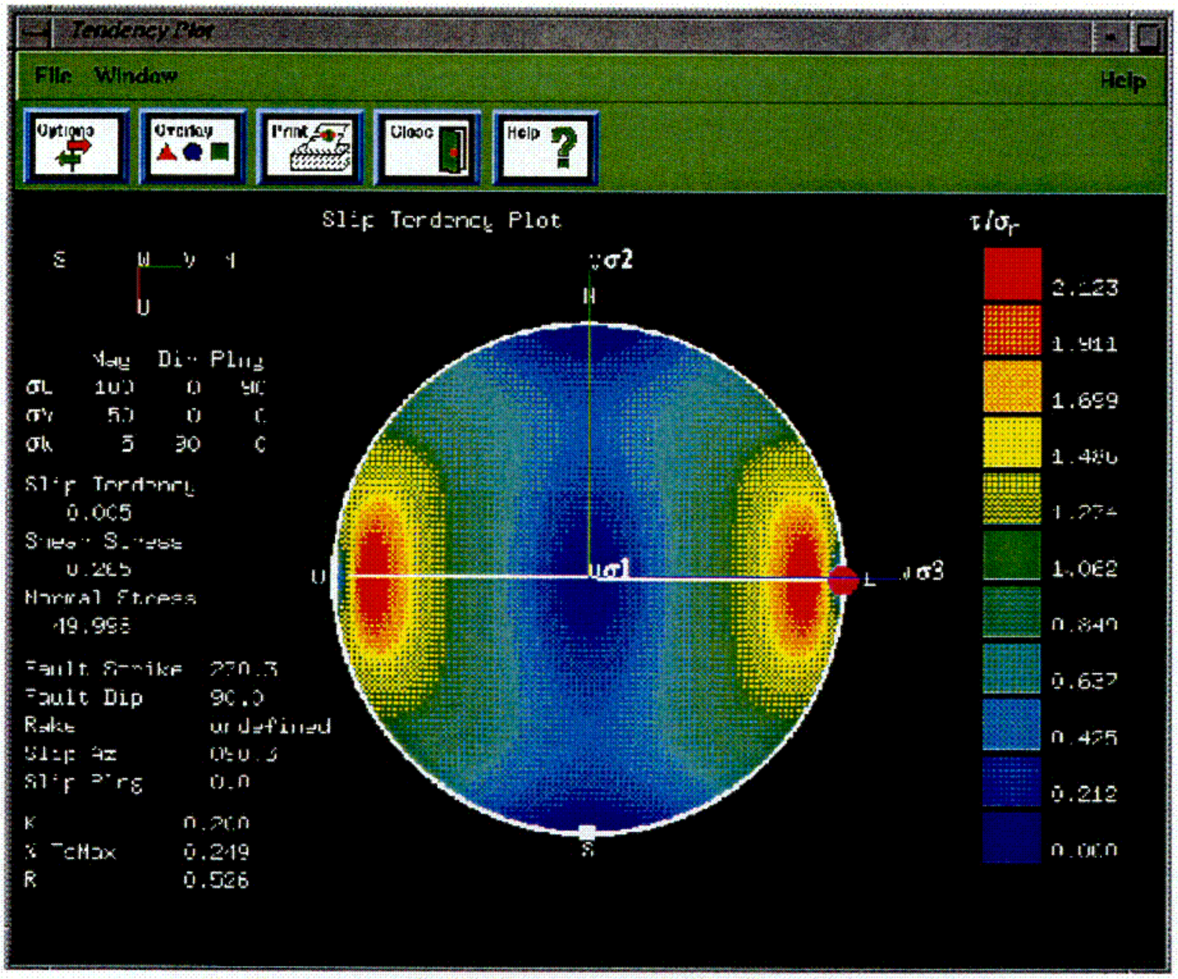

C04

The Controller

The 3DStress controller is used to access each of the main windows by clicking the left mouse button over the desired button.

	Tendency Plot	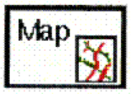	Map Viewer
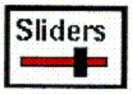	Magnitude Tool		Surface Viewer
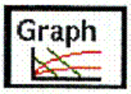	Stress Ratio Graph	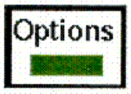	Options
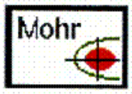	Mohr Graph	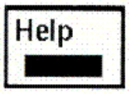	Help
	3D Fault Viewer		Exit 3DStress

C05

Common Buttons

Each of the different main windows accessed from the Controller has buttons located near the top of the window that serve a common purpose.

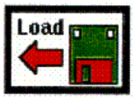

Load a file

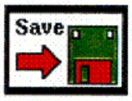

Save loaded file(s)

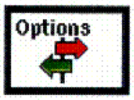

Options applying to that particular window

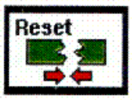

Centers the viewer and any loaded file(s)

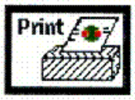

Saves the window to a screen raster file (bitmapped xwd format)

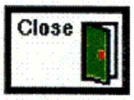

Closes the window

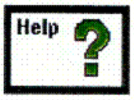

Help file for the window

C06

Tendency Plot

3DStress computes slip tendency based on a user-selected stress tate. The stress state is defined by the magnitudes and orientations of the orthogonal stress axes called σ_u, σ_v, and σ_w. The magnitude values in 3DStress are **normalized** to range from 1 to 100. These represent principal compressive stresses.

The stress axis with the **greatest** magnitude is called σ_1. The stress axis with the **smallest** magnitude is called σ_3. The **intermediate** stress axis is called σ_2. Any of the stress axes (σ_u, σ_v, or σ_w) can be σ_1, σ_2, or σ_3 depending on the user selection

A **stress state** is defined in terms of principal stress components σ_1, σ_2, and σ_3 ($\sigma_3 \leq \sigma_2 \leq \sigma_1$), which are oriented along orthogonal directions u, v, and w. The user may set the relative magnitudes of the principal stress components and may choose any two of the three orthogonal axes for σ_1 and σ_3. Initially, u points vertically down, but the user may rotate the stress axes to other orientations (see the Magnitude Tool section). Only mutually orthogonal stress-axis orientations are allowed by 3DStress.

Reading Slip Tendency and Direction Values

Slip tendency is displayed on a lower hemisphere equal-angle stereographic projection as shown below. Lo hemisphere plot correspond to fault surface poles. The slip tendency for a given fault pole is indicated on a indicates relatively high slip tendency and **blue** indicates relatively low slip tendency.

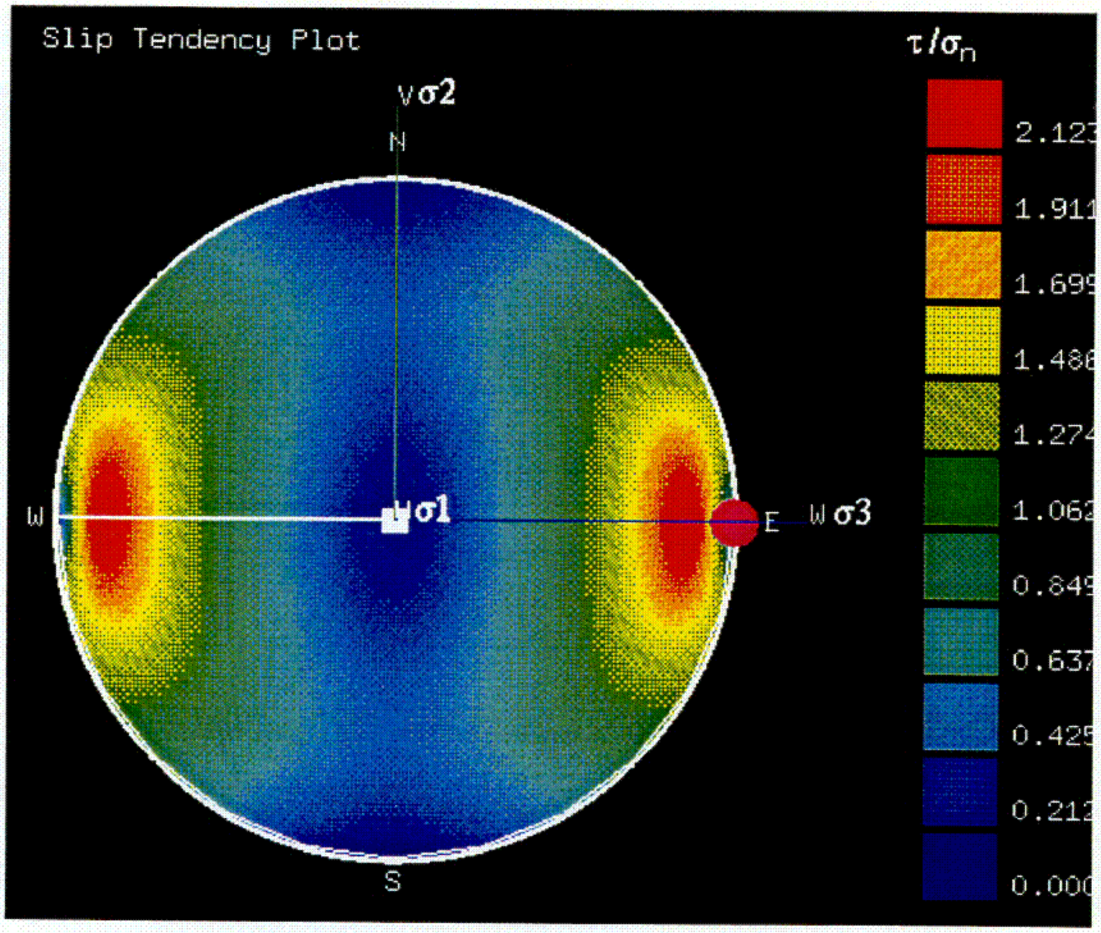

Slip is likely to occur on a surface when the resolved shear stress equals or exceeds the frictional resistance information see the references listed in the overview section.

Slip direction is shown as a purple dot on the lower hemisphere plot. Slip direction is always in the plane of to the fault pole, indicated by the white square. The user may select the fault pole by holding down the left moving the mouse over the lower hemisphere plot or by keyboard control. For keyboard control the **comma** control fault pole strike while the **n** and **m** keys control dip (for additional key controls see the appendix or on the tendency plot window).

C07

For further explanation of K, TsMax, and R see the **Stress Ratio Graph** section.

$$\%TsMax = \frac{\text{Slip Tendency for a select fault orientation}}{\text{Max Slip Tendency for all fault orientations in the current stress state}}$$

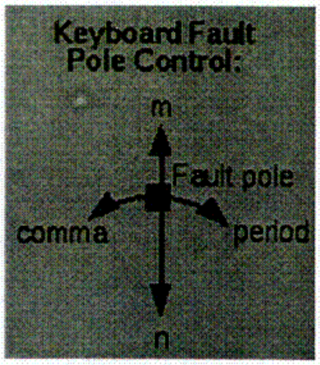

C08

Tendency Plot Options

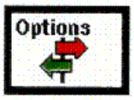

The **display** option allows rendering of the plot using either a **solid** shading, colored **lines**, or colored **points** as shown below.

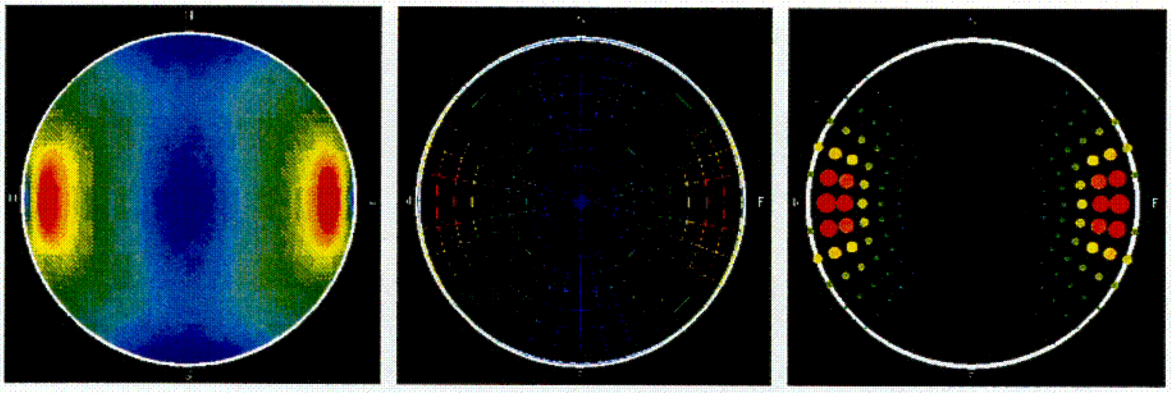

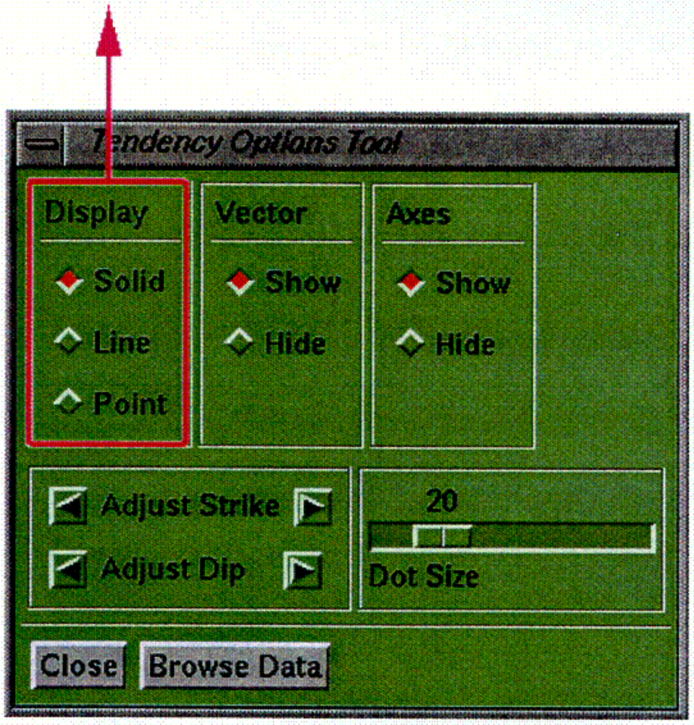

page 2

C09

The vector show and hide button controls the slip vector data display as shown below.

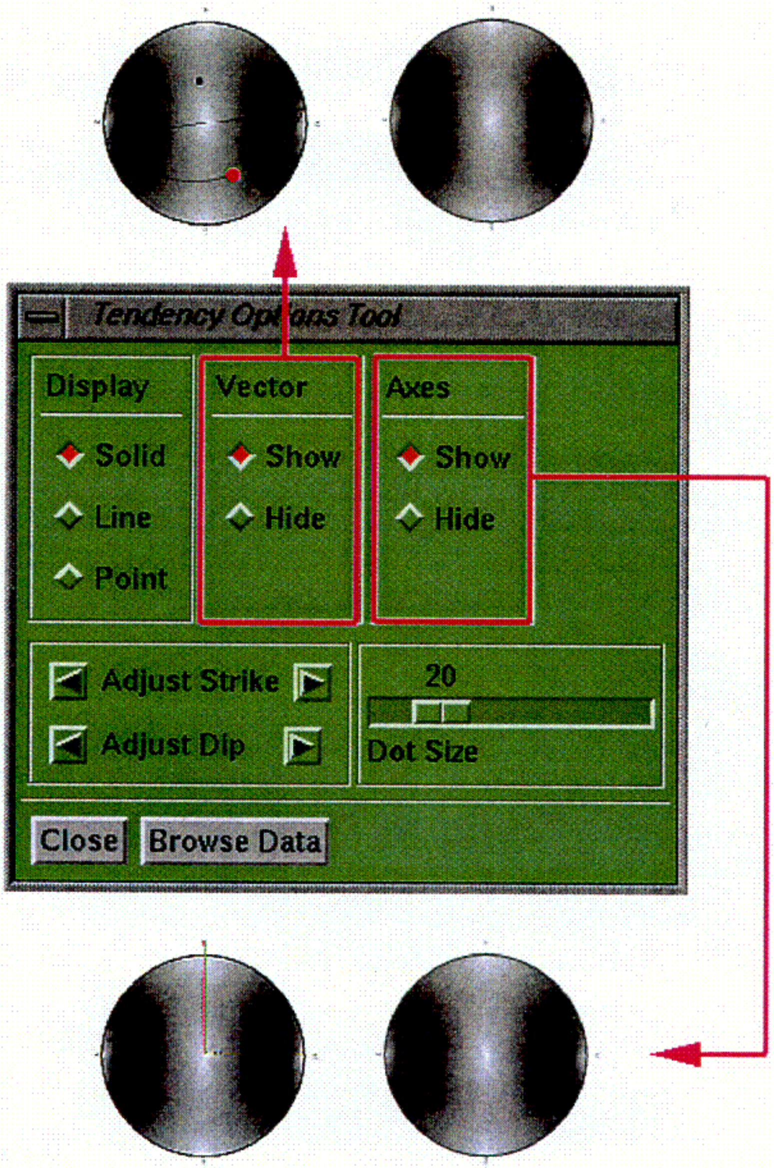

The axes show and hide button controls the plot axes display as shown above.

page 1 page 3

C10

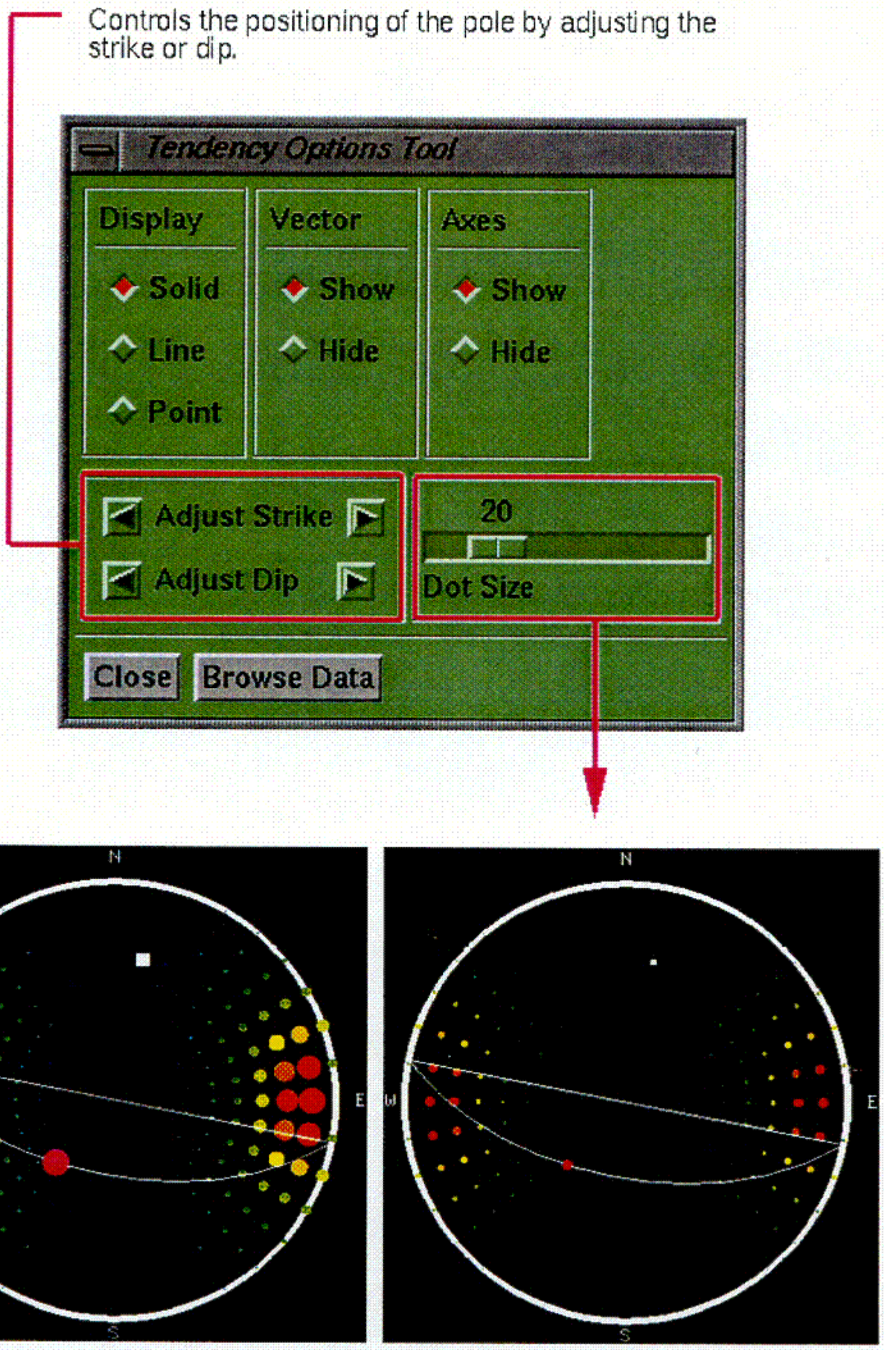

The **dot size** slider is only used with the display point mode as shown above.

page 2

Overlaying Points on the Slip Tendency Plot

Measured or pre-computed fault pole and slip vector data points may be displayed over the lower hemisphere plot. This enables comparison of measure or pre-computed data with the user selected stress conditions. Measured or pre-computed data sorted in an ASCII data file with the following format may be displayed with 3DStress.

```
# Comment lines begin with a "#" symbol
# Strike / dip
45 65
90 65
135 65
180 65
225 65
270 65
315 65
0 65
```

Numbered in the order they appear above, data is plotted according to the right hand rule.

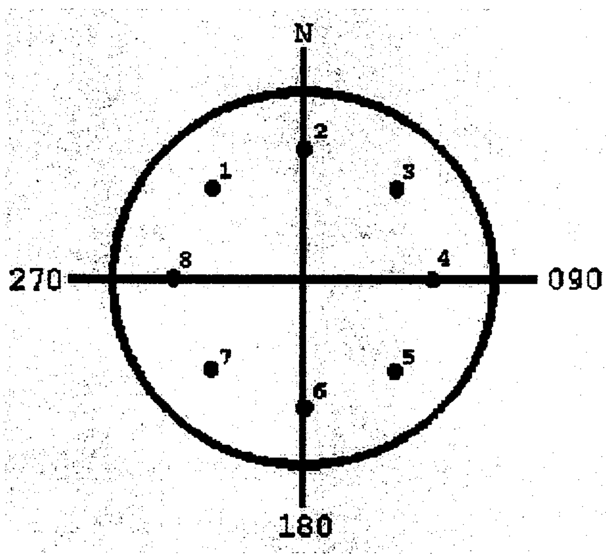

page 2

Overlay files are expected to have a file name extension of "ovr". Each overlay file may contain 1 or more data points. Multiple overlay files may be displayed simultaneously with 3DStress.

Overlays are handled by the Overlay Tool, which is displayed by pressing the overlay button on the Tendency Plot.

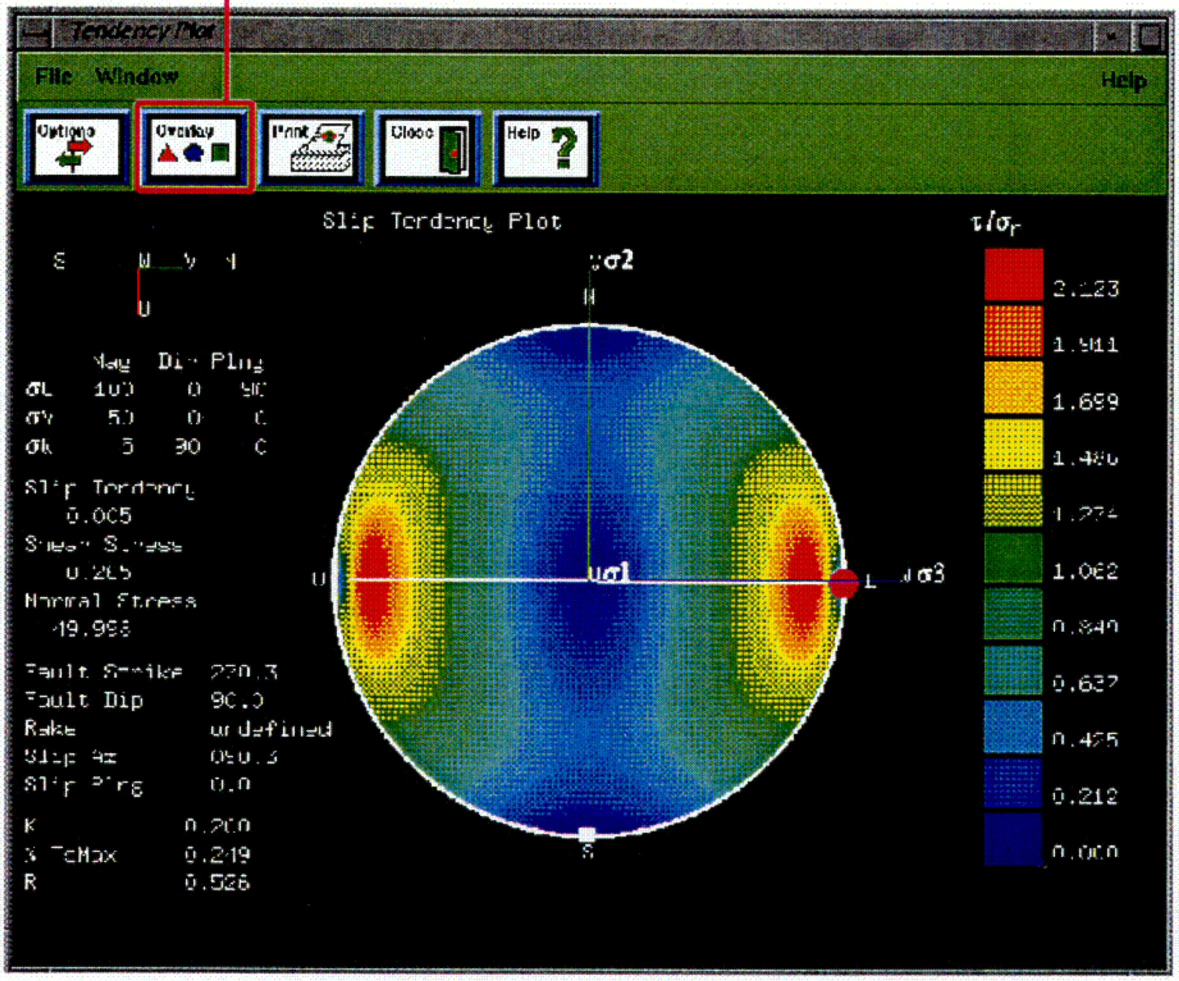

page 1 page 3

To load an overlay file, press the **Load** button and a file selector will appear. After selecting an overlay file, the name of the file is displayed in the Overlay Tool. Each loaded overlay may be manipulated by clicking on the overlay name, then adjusting the color sliders or clicking on one of the various shapes. Removal is done in a similar fashion by selecting an overlay and pressing the **Remove** button.

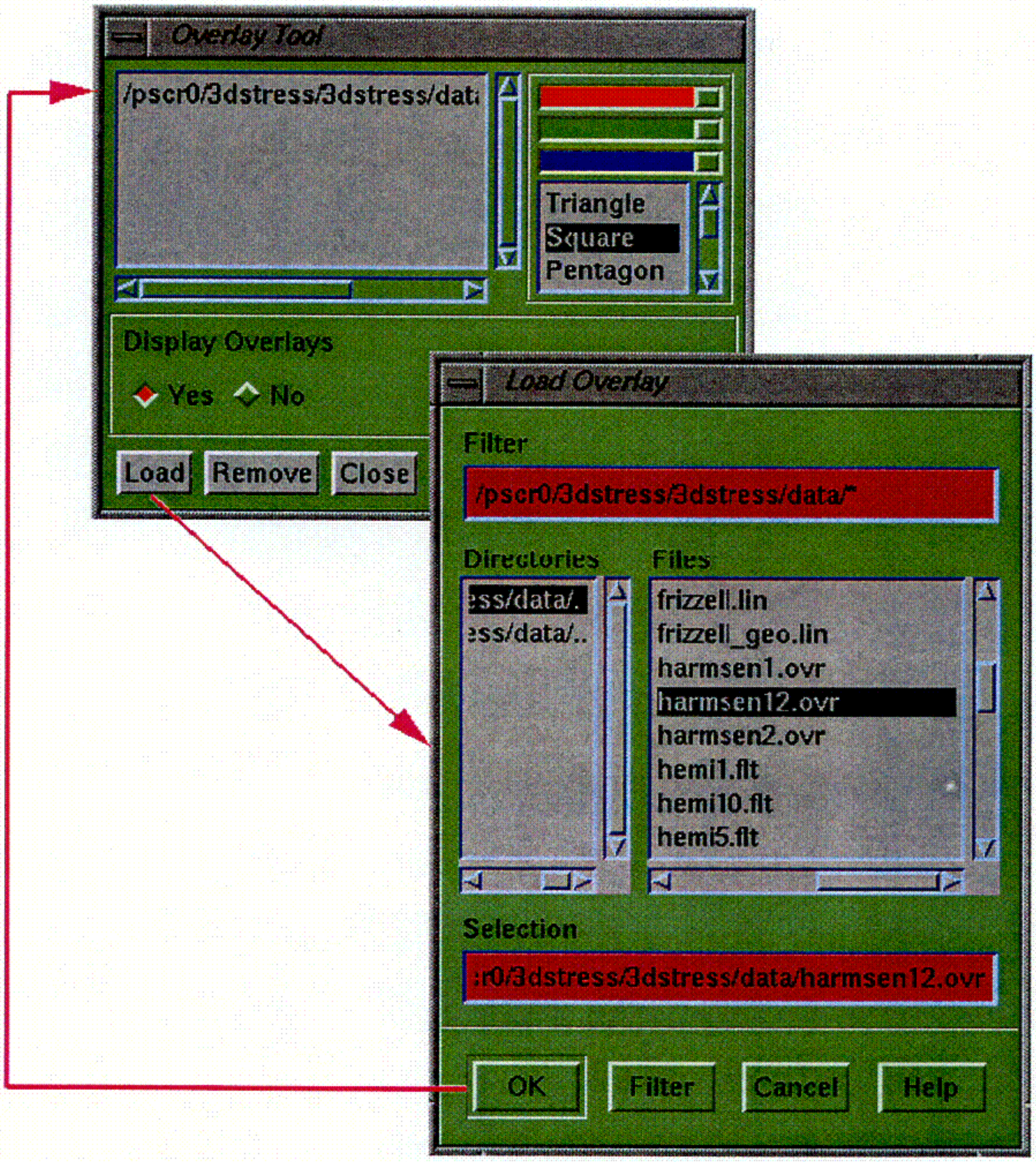

page 2 page 4

C13

Overlay data will appear as colored polygons on the lower hemisphere plot. All the points from a given overlay file will have the same color. Overlay data may represent fault poles or slip vectors. For example, one of the overlay datapoints (red triangle) below is located near the current slip vector (purple circle). Clicking on an overlay with the right mouse button displays the overlay file name.

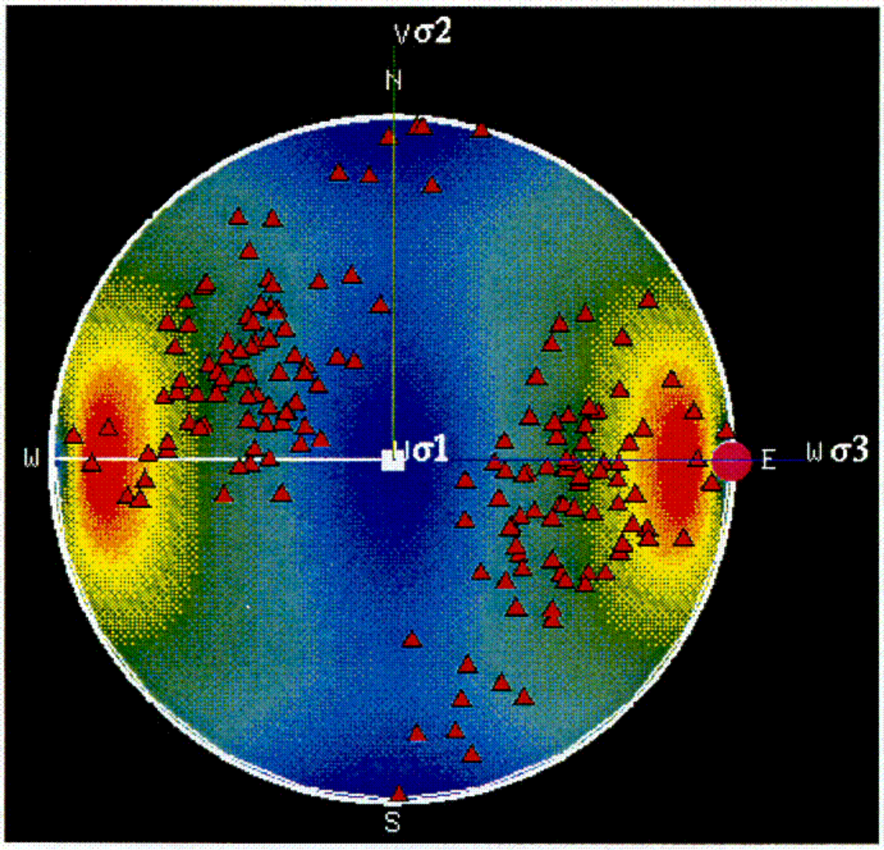

page 3

C14

Magnitude Tool

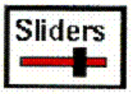

Stress magnitudes can be modified by using either the left or middle mouse button to select the desired normalized magnitude on the stress magnitude sliders. Input magnitudes range from 1 to 100 on each slider.

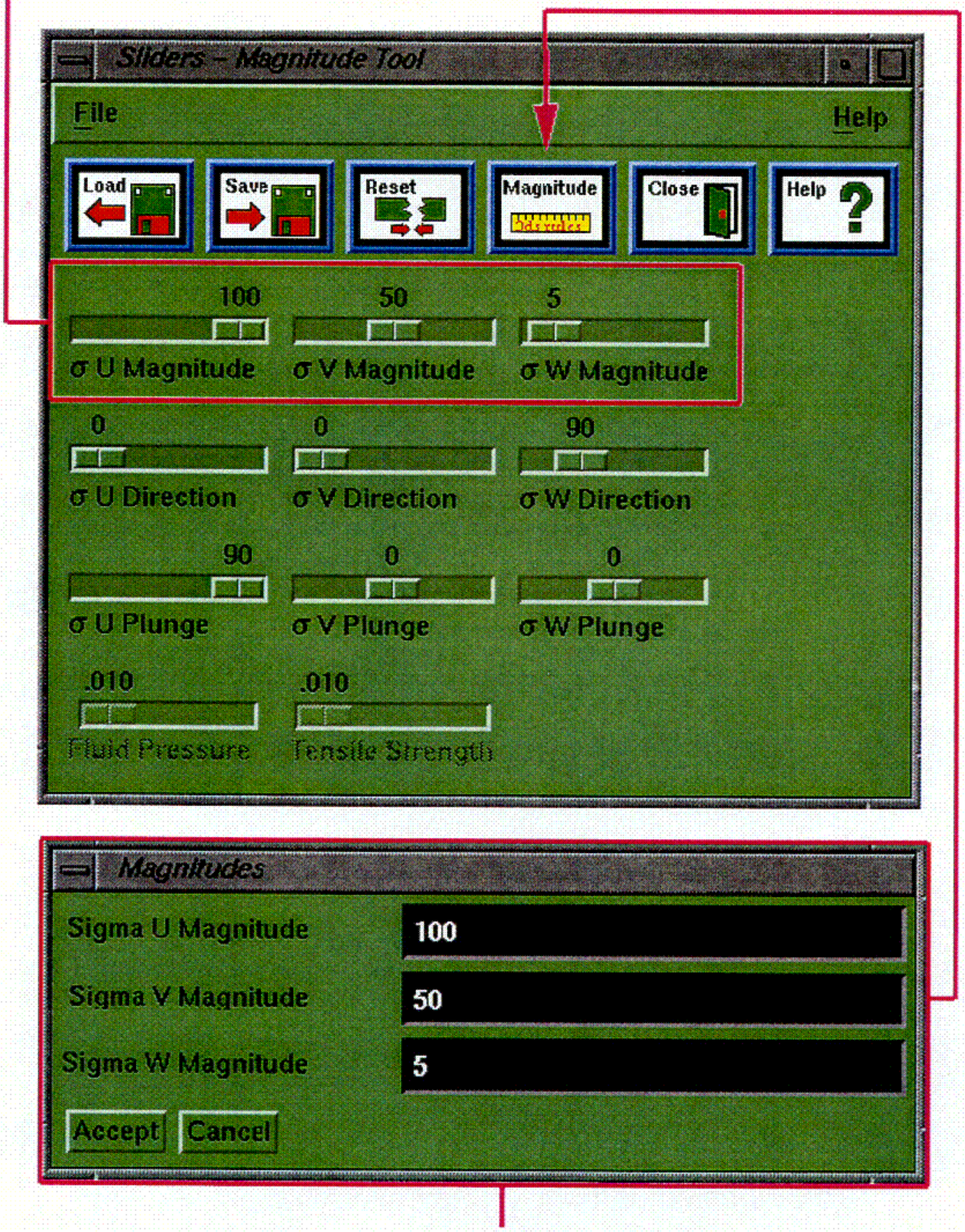

Use the magnitudes entry window to enter true magnitudes from the keyboard. The program will automatically normalize the input values to range from 1 to 100 while maintaining the correct magnitude ratios.

C15

Stress orientations are shown in degrees and are selected by using the left and middle **mouse buttons** with the orientation control **sliders**. The labels of the first axis selected will turn red. The **direction** and **plunge** of the **first-selected axis** may be entered. Only **direction** changes are allowed for the **other two axes**. Pressing the reset button will **reset** the orientations and allow selection of a new first-selected axis. Directions range from 0 to 360 and plunges range from 0 to 90 in order to enable any measured or simulated 3D stress orientation.

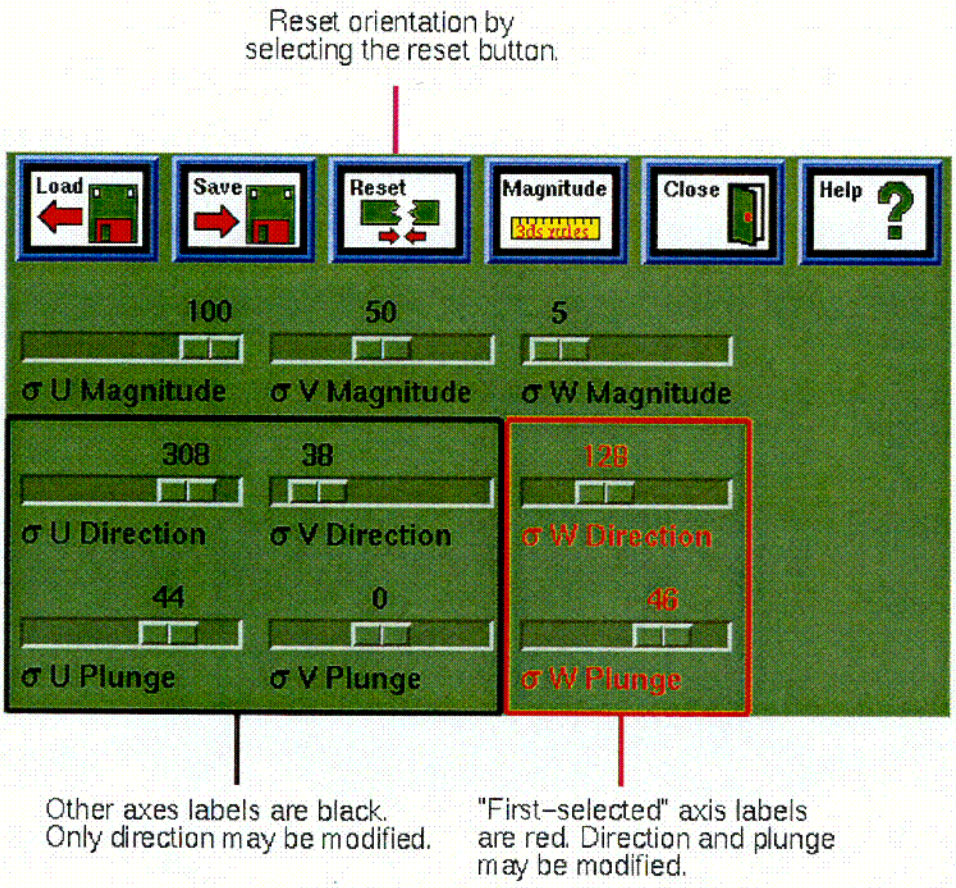

Fluid pressure and tensile strength may be used when computing leakage factor (see options).

Values are changed by using the left and right mouse buttons.

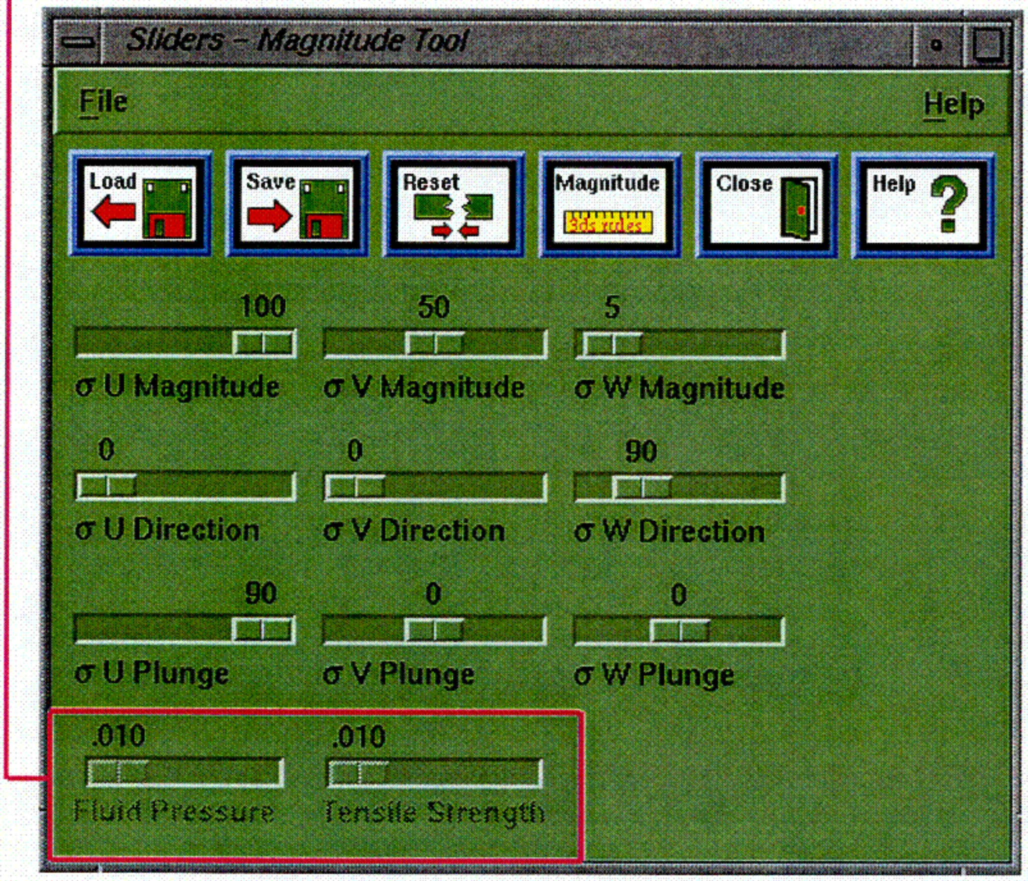

C17

Stress magnitudes and orientations may be saved by pressing the save button and specifying a file name. These values may then later be reapplied by using the load button and choosing a file.

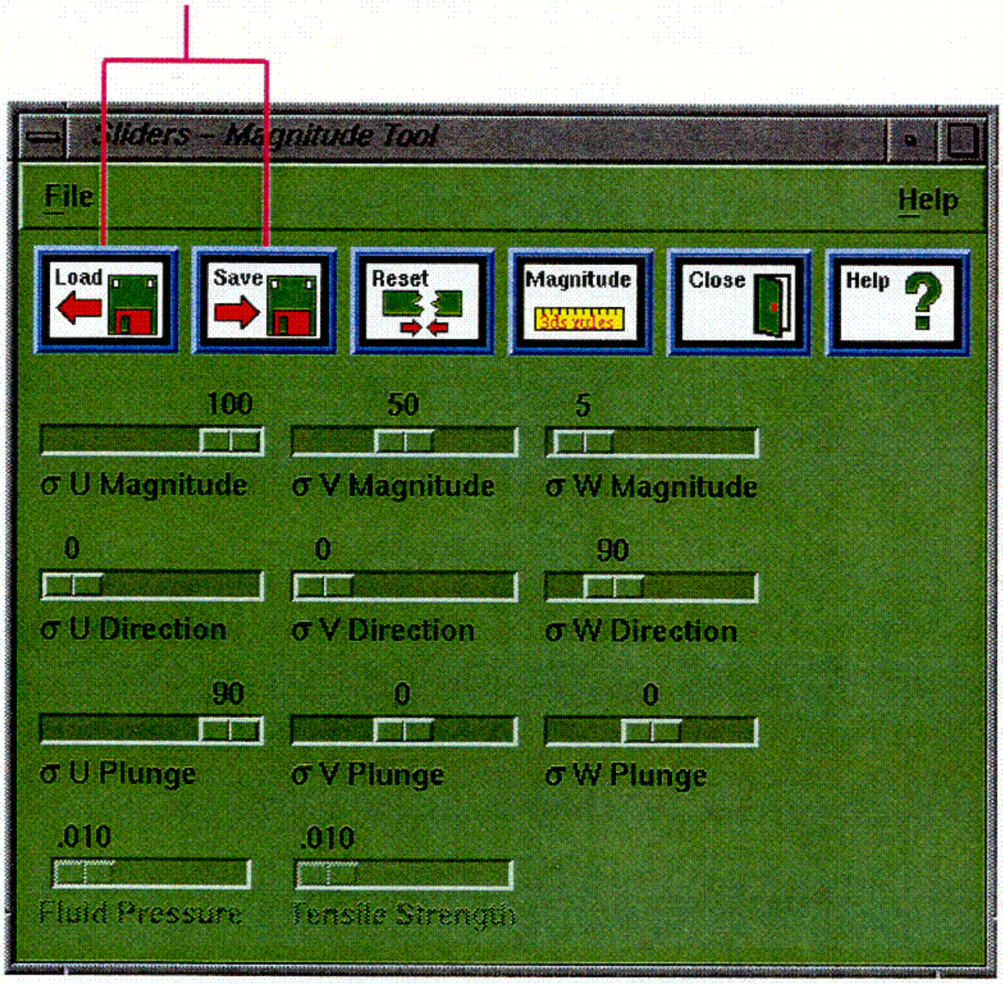

Stress Ratio Graph

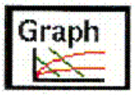

Use the stress ratio graph window to select the desired stress magnitude ratios by holding down the **left mouse button** and moving the cursor to the desired stress state and releasing the mouse button. The **right mouse button** toggles between a logarithm base 10 (log-log) and natural logarithm (ln-ln) scale.

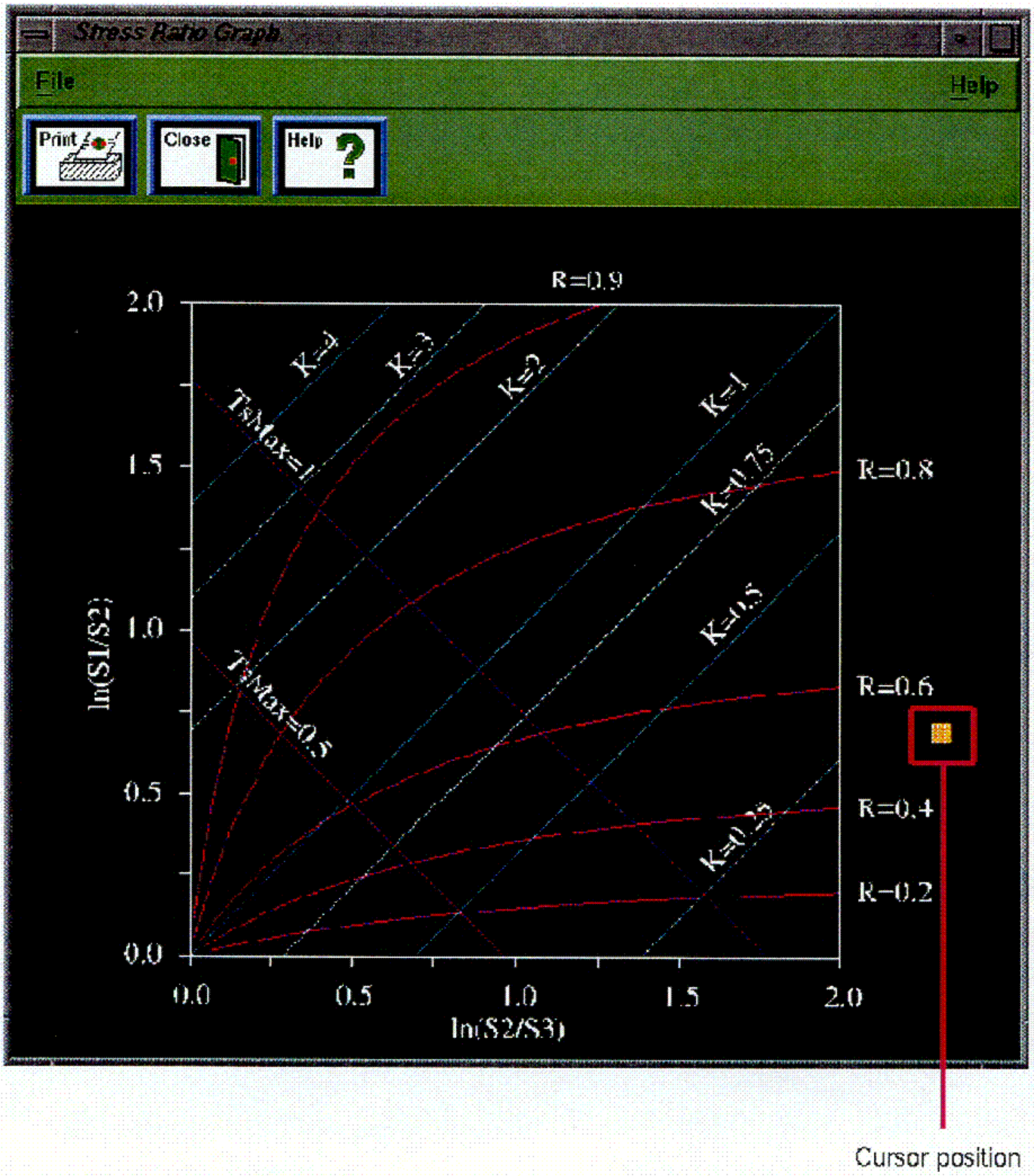

C19

page 2

The stress ratio graph displays a **yellow square** whose location is based on the stress ratios of σ_1 to σ_2 along the y-axis and σ_2 to σ_3 along the x-axis of the plot. σ_1 is the magnitude of the maximum principal stress, σ_2 is the intermediate principal stress, and σ_3 is the minimum principal stress. In addition to showing the location of the current stress state on a logarithmic scale, the graph also shows where the current stress state lies relative to plots of the following parameters:

$$K = (\sigma 1 / \sigma 2) / (\sigma 2 / \sigma 3)$$

$$R = (\sigma 1 - \sigma 2) / (\sigma 1 - \sigma 3)$$

TsMax = maximum slip tendency of all fault orientations for a given stress state.

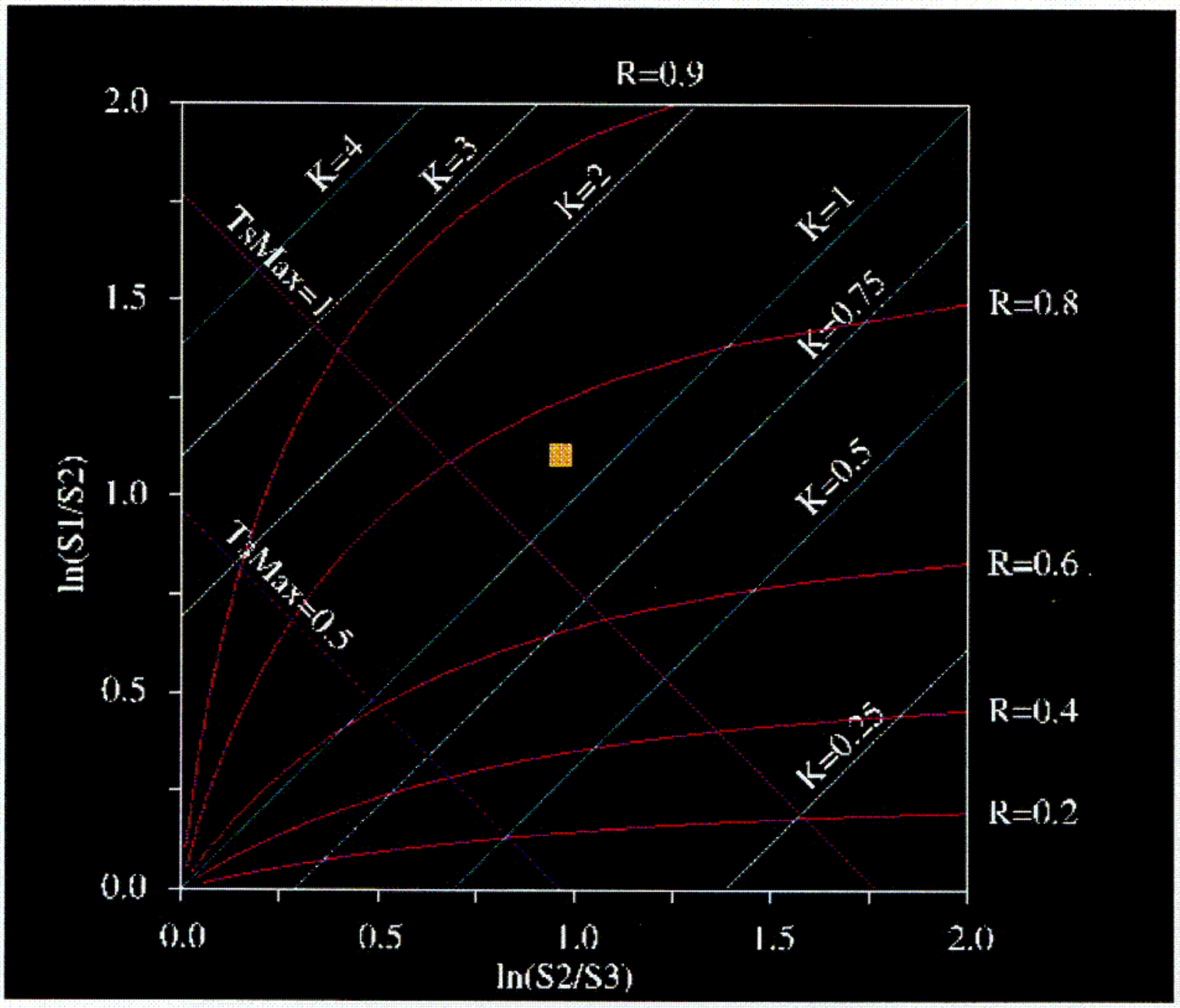

page 1 page 3

Natural logarithm scale

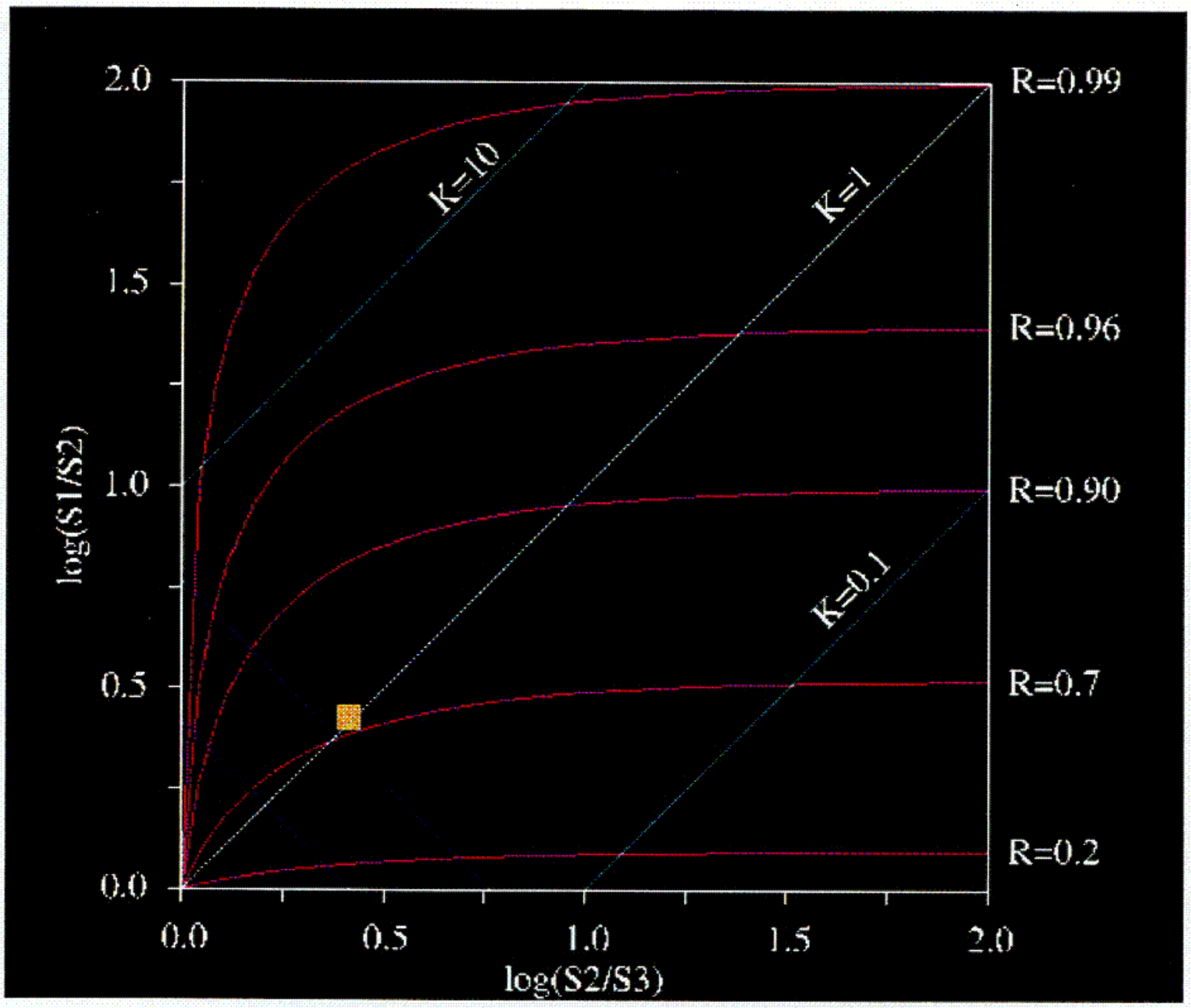

page 2

C21

Mohr Graph

The Mohr Graph allows the user to apply stress and fluid pressure to a specified type of rock and visualize the result. The result of the stresses and fluid pressure on the rock is displayed in a traditional Mohr Graph. Effective stresses are indicated in the visual display by an asterisk.

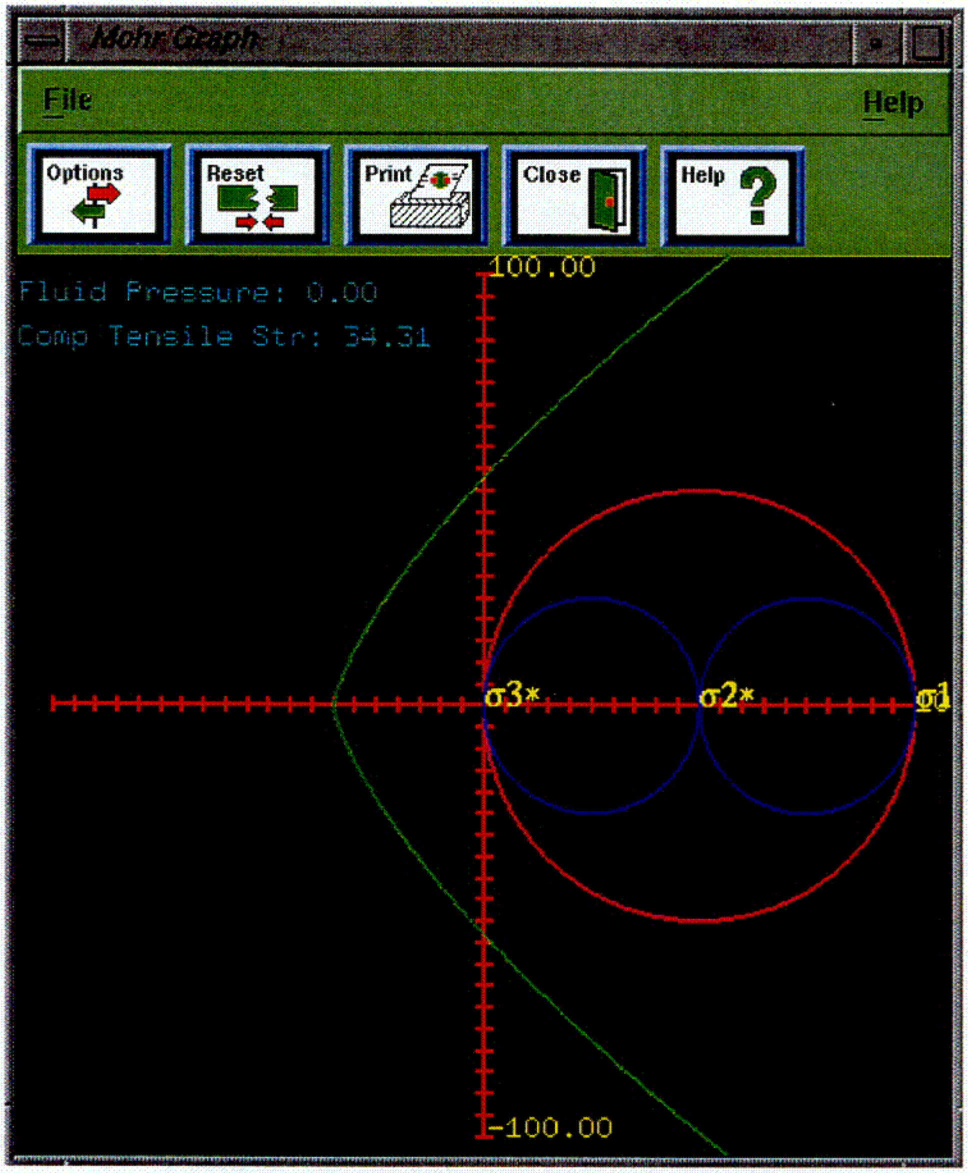

page 2

C22

The rock attributes may be altered in the Hoek-Brown Strength portion of the Options window.

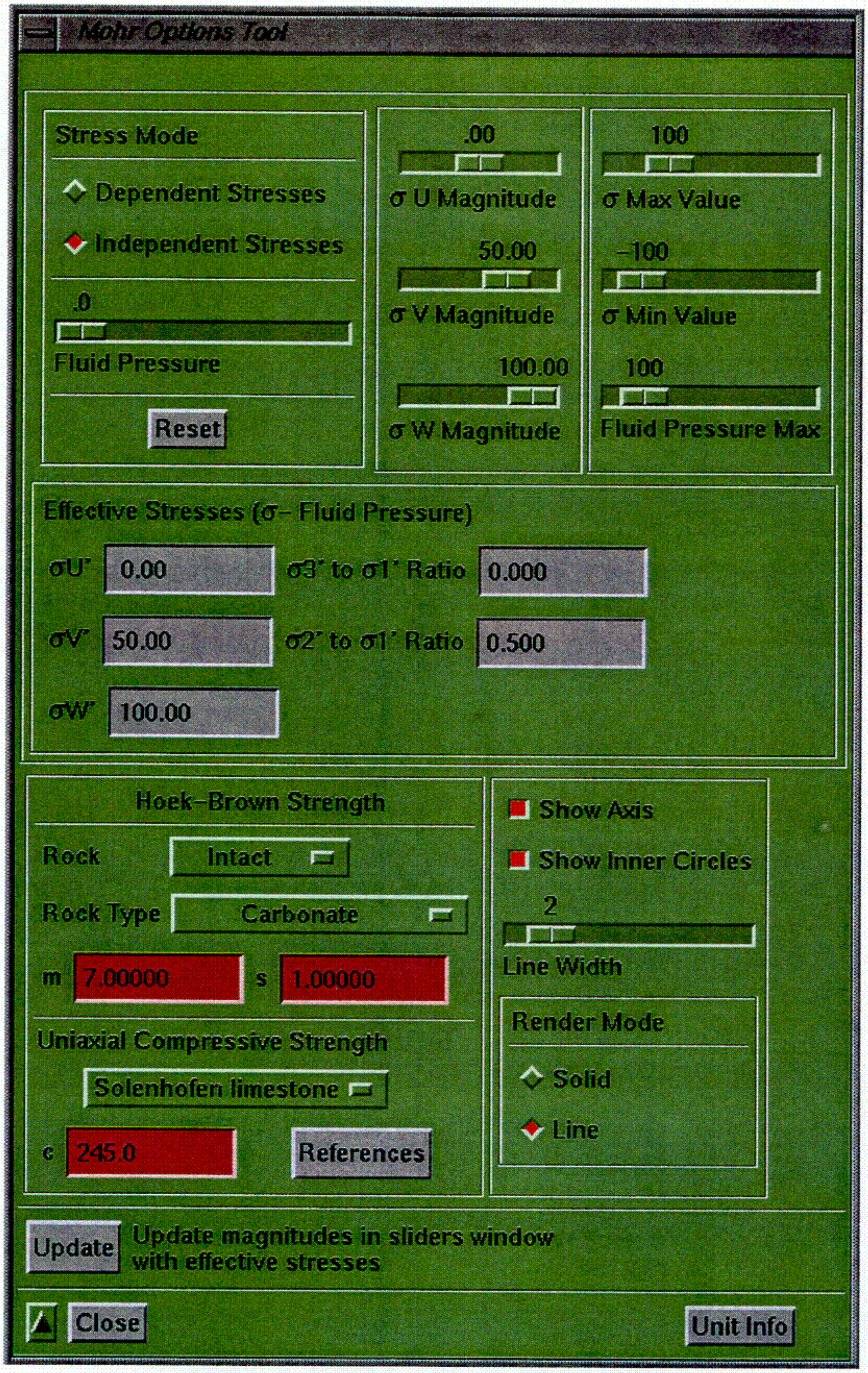

page 1 page 3

C23

In particular, the user may enter the quality, material type, and specific rock test results to work with pull down menus. The variables m, s, and c may be entered via text fields.

Another interesting feature of the 3DStress Mohr Graph is the ability to switch between dependent and independent stress modes. When Dependent Stress Mode is selected, sliders and text boxes for the specification of the stress ratios appear.

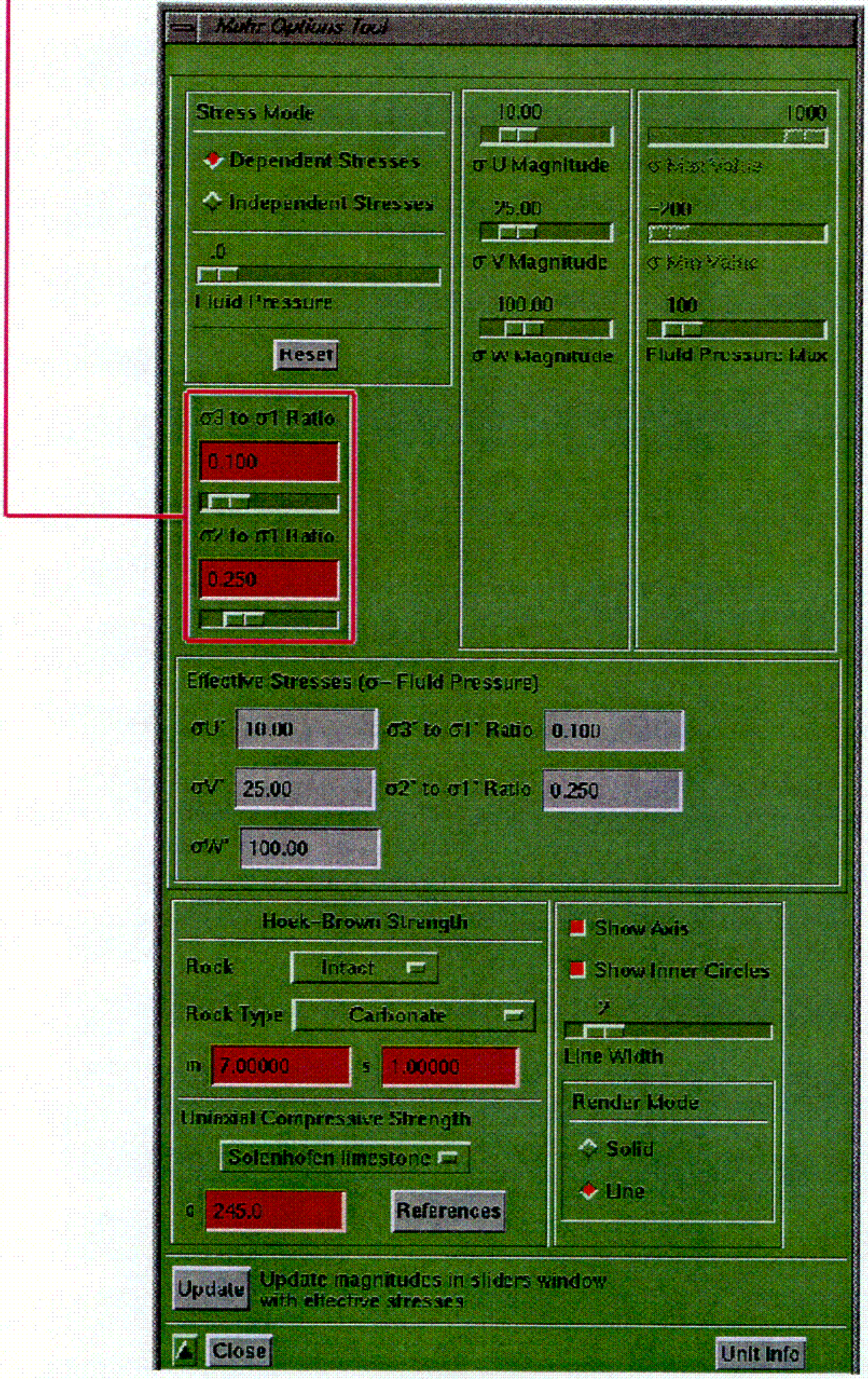

24

page 2

3D Fault Viewer

The 3D Fault Viewer enables the user to view and interact with faults defined in 3-space as polygons. The following formats for input files are currently supported: flt, vbl, and 3ds. The 3ds file format is the 3DStress application's own specific format not to be confused with the popular three-dimension modeling mesh format.

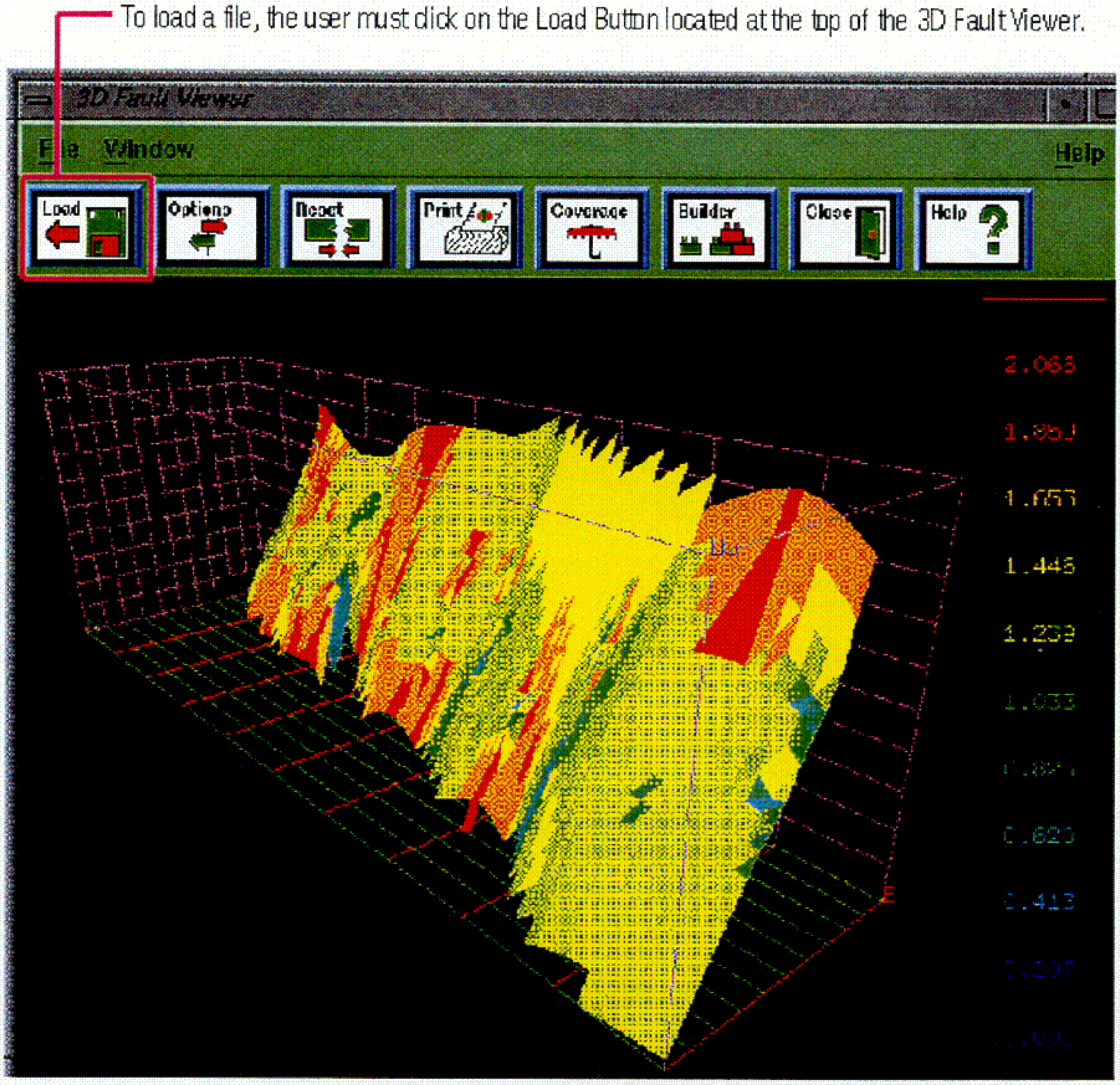

Upon clicking load, the user will be prompted with a file browser dialog window with which the file may be selected.

page 2

C25